4-Hydroxy-3-nitro-5-ureido-benzenesulfonamides selectively target the tumor-associated carbonic anhydrase isoforms IX and XII showing

4-Hydroxy-3-nitro-5-ureido-benzenesulfonamides selectively target the tumor-associated carbonic anhydrase isoforms IX and XII showing hypoxia-enhanced anti-proliferative profiles.

Alessio Nocentini[a],* Elena Trallori[b], Srishti Singh[c], Carrie L. Lomelino[c], Gianluca Bartolucci[a], Lorenzo Di Cesare Mannelli[b], Carla Ghelardini[b], Robert McKenna[c], Paola Gratteri[a,]*, Claudiu T. Supuran[a,]*

[a]*Università degli Studi di Firenze, NEUROFARBA Dept., Sezione di Scienze Farmaceutiche, Via Ugo Schiff 6, 50019 Sesto Fiorentino (Florence), Italy*

[b]*Department of Biochemistry and Molecular Biology, College of Medicine, University of Florida, Box 100245, Gainesville, FL 32610, USA*

[c]*Department of NEUROFARBA-Pharmacology and Toxicology Section, University of Florence, 50019 Florence, Italy*

Abstract

Human carbonic anhydrases (CA, EC, 4.2.1.1) IX and XII are overexpressed in cancer cells as adaptive response to hypoxia and acidic conditions characteristic of many tumors. In addition, hypoxia facilitates the activity of specific oxido-reductases that may be exploited to selectively activate bio-reductive prodrugs. Here, new selective CA IX/XII inhibitors, as analogues of the anti-tumor phase II drug **SLC-0111** are described, namely ureido-substituted benzenesulfonamides appended with a nitro-aromatic moiety to yield an anti-proliferative action increased by hypoxia. These compounds were screened for the inhibition of the ubiquitous hCA I/II and the target hCA IX/XII. Six X-ray crystallographies with CA II and IX/mimic allowed for the rationalization of the compounds inhibitory activity. The effects of some such compounds on the viability of HT-29, MDA-MB-231 and PC-3 human cancer cell lines in both normoxic and hypoxic conditions were examined, providing the initiation towards the development of hypoxia-activated anti-tumor CAIs.

Keywords: Hypoxia, tumor-associated carbonic anhydrase, inhibition, anti-proliferative.

Introduction

Hypoxia is a condition characterized by low levels of oxygen that commonly marks the microenvironment within solid tumors. Hypoxia results from dysfunctional microvasculature caused by the rapid growth of the tumor.[1-3] As such, hypoxia promotes several effects in the tumor, including a switch to glycolytic metabolism,[4-5] extracellular acidosis,[6] resistance to apoptosis,[7] increased mutation upon inhibition of DNA repair,[8] up-regulation of angiogenesis,[4] enhanced local invasiveness,[6] metastatic spread,[3] and promotion of cancer cells stemness.[9] The hypoxia-inducible factor 1 (HIF-1) programs such an orchestra of events, which results in cancer cells survival and proliferation.[4] Additionally, tumor hypoxia plays a role in resistance to radiotherapy and chemotherapy.[10] As a result, the hypoxic microenvironment of solid tumors has become of interest to the scientific community for the development of novel anti-cancer agents.

Since the majority of normal tissues are devoid of hypoxic regions (although mild physiological hypoxia can be found in several tissues), bio-reductive prodrugs can be designed for selective activation under low oxygen conditions typical of many solid tumors.[3,11] Hypoxia-activated prodrugs (HAP) are designed to target and kill hypoxic cells.[12-14] The enzymes responsible for the activation of these prodrugs include a variety of specific one-electron and two-electron oxido-reductases (e.g. POR), whose catalysis differs depending on the bioreductive drug class. Inhibition of this process by molecular oxygen imparts specificity for the hypoxic tumor regions and ensures that the bio-reductive drugs exhibit a reduced toxicity to normal tissues. The majority of HAP metabolites lead to DNA damage by interfering with DNA replication.[12-14]

Among the five identified classes of bioreductive compounds that can undergo enzymatic reduction to active species, several nitro-aromatic derivatives (which also constitute important therapeutic agents against a variety of protozoan and bacterial infections of humans and animals) have been evaluated in clinical trials,[12-14] including the nitroimidazoles developed for hypoxic cell imaging using immuno-histochemistry or positron emission tomography (PET).[15] Thereafter, reduction of a nitro group (NO_2) to a hydroxylamine (NHOH) or amine (NH_2) moiety has been utilized to design

the hypoxic cytotoxin **PR-104** (in phase II clinical trials), whose cytotoxic metabolites give rise to DNA interstrand cross-links, which can kill tumor cells.[16-17]

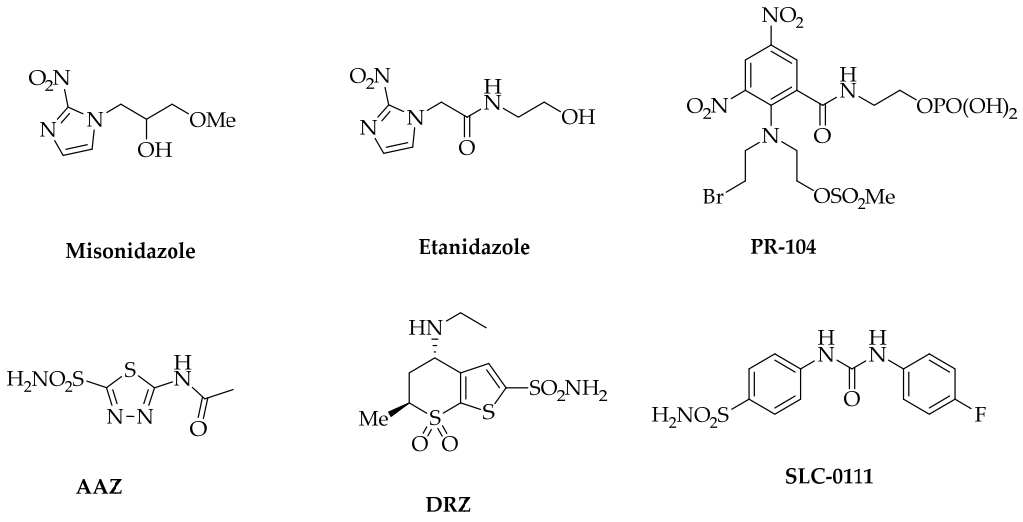

Figure 1. Structures of nitroaromatic HAPs, clinically used CAIs and **SLC-0111** the sulfonamide CA IX/XII inhibitor in Phase I/II clinical trials.

Two isoforms of carbonic anhydrase (CAs, EC 4.2.1.1), CA IX and CA XII, are overexpressed in hypoxic cancers and contribute to tumor physiology by supporting an acidic extracellular microenvironment suited for hypoxic tumor cell survival and proliferation, but detrimental to normal cells.[18-20] Particularly, CA IX is normally expressed in few tissues, but is upregulated in many tumor types (e.g. colorectal, breast, brain, etc.) mainly due to its strong transcriptional activation by hypoxia mediated by the HIF-1 transcription factor.[20] CA IX and XII have been validated as markers of disease progression in many hypoxic tumors and their targeted inhibition has been associated with a significant reduction of the growth of both primary tumors and metastases.[6] Hence, these CA isoforms have become attractive targets for the design of anti-neoplastic therapies, as recently proposed by several groups. Not surprisingly, CA IX/XII have been the main focus of the last decade research over other CA isoforms.[6,18-20]

CA IX and XII are transmembrane, multi-domain proteins whose extracellular catalytic domain is similar to that of the other cytosolic, mitochondrial, secreted or membrane-anchored hCA isoforms.[21,22] Ubiquitous cytosolic isoforms CA I and II are the main off-target isoforms when CA

IX and XII are the targets. Primary sulfonamides are the most investigated class of CAIs and have been in clinical use for almost 50 years for the treatment of glaucoma, epilepsy, and as diuretics. Acetazolamide (**AAZ**) and Dorzolamide (**DRZ,** Figure 1) are the prototypical first, and second-generation drugs.[19] Their lack of selectivity amongst the human CA isoforms is a major issue in the therapeutic anti-tumor applications of CA IX/XII sulfonamide-based inhibitors, due to the risk of unwanted side effects.[18,23]

The lead methods that have been applied for the identification of isoform selective sulfonamide-based CAIs are the ring and the tail approach, which respectively consist of modulating a ring (mainly its chemical nature) directly linked to the sulfonamide group and appending different tails to the aromatic/heterocyclic ring present in the scaffold of the CAIs.[24-27] In particular, this allows the modulation of interactions with the variable active site regions present towards the middle and the edge of the CAs binding sites.[18]

Extensive application of the tail approach, over the last decades, has greatly enriched the database of CAIs, although only a small subset of CA isoform-selective derivatives was found. Linkers of the ureido-type stood out amongst a plethora of available functional groups for ease of preparation, increased water solubility of derivatives and high flexibility of the spacer.[28-32] For these reasons, incorporation of linkers of the ureido-type have been widely pursued for sulfonamides and their bioisoster sulfamates, leading to several CAIs with selective inhibition profiles for the tumor-associated isoforms.[28-32]

Among such series of derivatives, **SLC-0111**, a simple, ureido-substituted benzenesulfonamide successfully completed Phase I clinical trials for the treatment of advanced, metastatic hypoxic tumors over-expressing CA IX and has been scheduled for Phase II trials later last year.[33]

Previous studies have reported hypoxia-activated sulfonamides incorporating disulfide functionalities, as well as a series of 3-nitro-2-substituted benzenesulfonamides, with the aim of designing bio-reductive inhibitors targeting the hypoxia regulated, tumor-associated isozymes, but *in vitro/vivo* studies of these compounds were not reported.[34,35] Rami et al. reported a series of

nitroimidazoles incorporating sulfonamide-like moieties as radio/chemosensitizing agents targeting the tumor-associated CA IX and CA XII.[36]

Here we explore the possibility of designing selective CA IX/XII inhibitors of the ureido-substituted benzenesulfonamide-type incorporating a nitro-aromatic moiety to yield a cytotoxic effect increased by hypoxia. The derivatives were obtained from 3-nitro-4-hydroxy-5-aminobenzenesulfonamide that was procured by a selective mono-reduction of the di-nitro precursor. The series of compounds was screened for the inhibition of the physiologically relevant CA isoforms I, II, and the tumor-associated CA IX and XII. X-ray crystallography was employed for rationalizing the CA inhibitory profiles and the adduct of three inhibitors with both CA II and IX/mimic analysed at the molecular level. A hypoxia-enhanced anti-proliferative activity of some such derivatives, albeit not striking, was shown by studying their effects on viability of human colorectal HT-29, breast adenocarcinoma MDA-MB-231, prostate PC-3 cancer cell lines in both normoxic and hypoxic conditions.

Result and Discussion

Chemistry

The derivatives were firstly designed to selectively inhibit CA IX and XII over the cytosolic I and II. Thus, the incorporation of the nitro group should be considered from the structure-activity relationship point of view. The nitro group represents a unique functional group with a variety of chemical and biological actions. Its strong electro-withdrawing nature creates localized or regional electron deficient areas within the molecules.[37] Appending a nitro group at the benzenesulfonamide scaffold might be considered as an application of the ring approach in that the chemical nature of the main scaffold is influenced. Overall, the acidity of the sulfonamide group is enhanced. In addition, the nitro moiety can participate in both intermolecular and intramolecular hydrogen bonding, increasing the possible interaction points within the binding site pockets.[37]

Of note, Mori et al. recently reported a series of nitro-benzoic acid as potent and selective CA IX and XII inhibitors, although the carboxy moiety generally has worse CA inhibition properties than the sulfonamide group.[38]

A structural development of **SLC-0111** recently reported by us led to the identification of new promising CA IX/XII selective ureido-CAIs. The compounds, of the **A** type (Figure 2), exhibit a tail incorporated in *meta* with respect to the sulfonamide moiety and an additional *para*-OH. The latter increases CAs enzymatic selectivity by rotational restriction of precise intramolecular bonds and enhances the derivatives water solubility.[39] The fluoro-phenyl derivative was investigated *in vivo* using an orthotopic syngeneic breast tumor model that robustly expresses hypoxia-inducible CA IX. It was found to inhibit tumor growth in a dose-dependent manner, reaching levels that matched those observed with **SLC-0111** treatment.[39]

Considering this evidence, the aim was to incorporate a nitro-aromatic moiety in an **A** type structure to yield additional anti-hypoxic tumor activities.

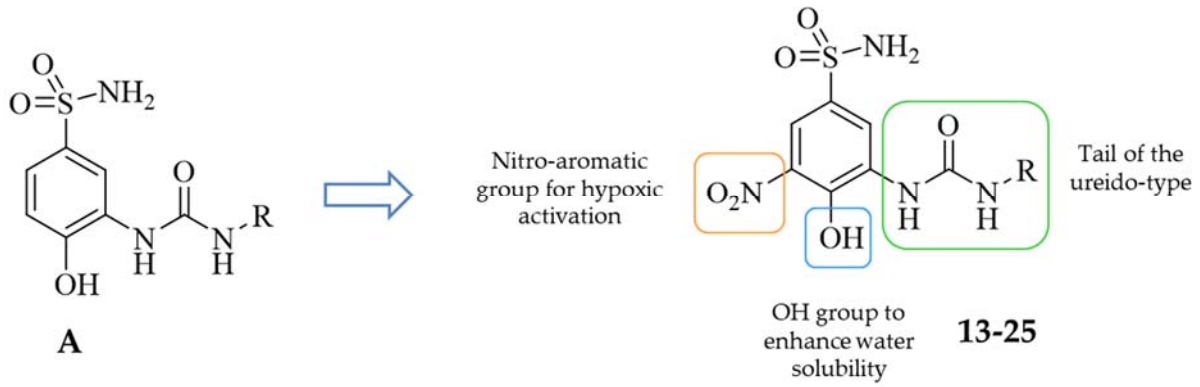

Figure 2. Design of 4-hydroxy-3-nitro-5-ureido-benzenesulfonamides.

To nitrate a benzenesulfonamide ring, it is important to consider the reactivity of the aromatic core as well as instability of other groups to the nitration conditions. Sulfonamide rapidly decomposes to sulfonic acid passing through N-nitrosulfonamide, requiring a proper protection that was afforded by using N,N-dimethylformamide diethyl acetal.[40]

Conversely, protection of aromatic amines with the latter reactant [41] or acetyl/Boc did not prevent decomposition in the nitrating mixture. As a result, the 3-amino-4-hydroxybenzenesulfonamide could not be used as a starting point in the synthetic strategies.

On the other hand, phenolic moieties are known to exhibit stability towards nitration[40] making it possible to the synthetic pathway with 4-hydroxybenzenesulfonamide. It should be considered that heating was necessary to achieve a dinitration of the aromatic scaffold since that is impaired by the benzene ring deactivation elicited by strong electron-withdrawing groups, such as the sulfonamide and first forming nitro moiety. For instance, attempts to di-nitrate the unsubstituted benzenesulfonamide crashed with the strong deactivation of the intermediate 3-nitrobenzenesulfonamide.

The synthetic routes planned to afford the main series of ureido-derivatives led to possible deviations from the main synthetic pathway, which were also explored to generate further SAR.

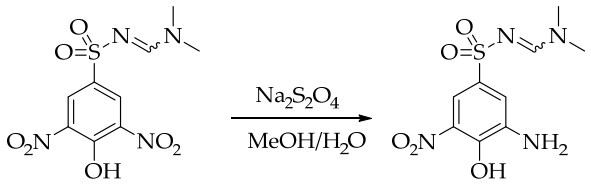

3 **7**

Reducing agent	Solvent	Yield %
Fe (0)	AcOH/EtOH/H_2O	36
NaHS	EtOH/H_2O	21
$Na_2S_2O_4$	MeOH/H_2O	47

Scheme 1. Employed methods to achieve the selective mono-reduction of di-nitro derivative **3** to aminophenol **7.**

The key intermediate 3-amino-4-hydroxy-5-nitro-benzenesulfonamide **8** was obtained by the di-nitration of the protected 4-hydroxybenzenesulfonamide **2**, followed by the reduction of a unique nitro group with formation of the amino phenol **7** (Scheme 1) and successive sulfonamide deprotection in acidic media. The attempt to directly nitrate the 4-hydroxybenzenesulfonamide **1** in

the sulfonitric mixture led to sulfonamide decomposition to the corresponding di-nitro sulfonic acid. Indeed, we recently reported a similar behavior in the synthesis of N-nitrosulfonamides.[40]

The mono-nitro derivative **3a** was also isolated in low yields and thus deprotected, which was taken into account for the *in vitro* assays. Diverse reducing agents and reactions conditions were investigated in order to afford the selective mono reduction of derivative **3**.[42-45] The better, although still low yields, were achieved when $Na_2S_2O_4$ was used according to the literature method.[42]

Derivative **3** was also deprotected in acidic media to give the primary sulfonamide **5.** The latter was used as the starting material for one of the previously mentioned deviations from the main synthetic pathway. Unfortunately, our aim to obtain a set of di-nitro esters crashed with the rather low stability of most such compounds.[46] Uniquely the benzoyl derivative **6** was obtained.

The key intermediate **8** was subjected to diverse functionalizations in addition to the originally planned ureas production.

First, acylation reactions of the amino group did not produce high yields of the planned amide derivatives. As a likely result of the strong acidity of the phenol group and the poor nucleophilicity of the amine, the di-benzoyl compounds **9** and **10** were obtained. The pyridinium salt **11** was prepared by the reaction of **8** with the proper pyrylium compound.[47] The light-sensitive derivative **12** was achieved by diazonium salt formation and N_2 release in aqueous $NaNO_2$.

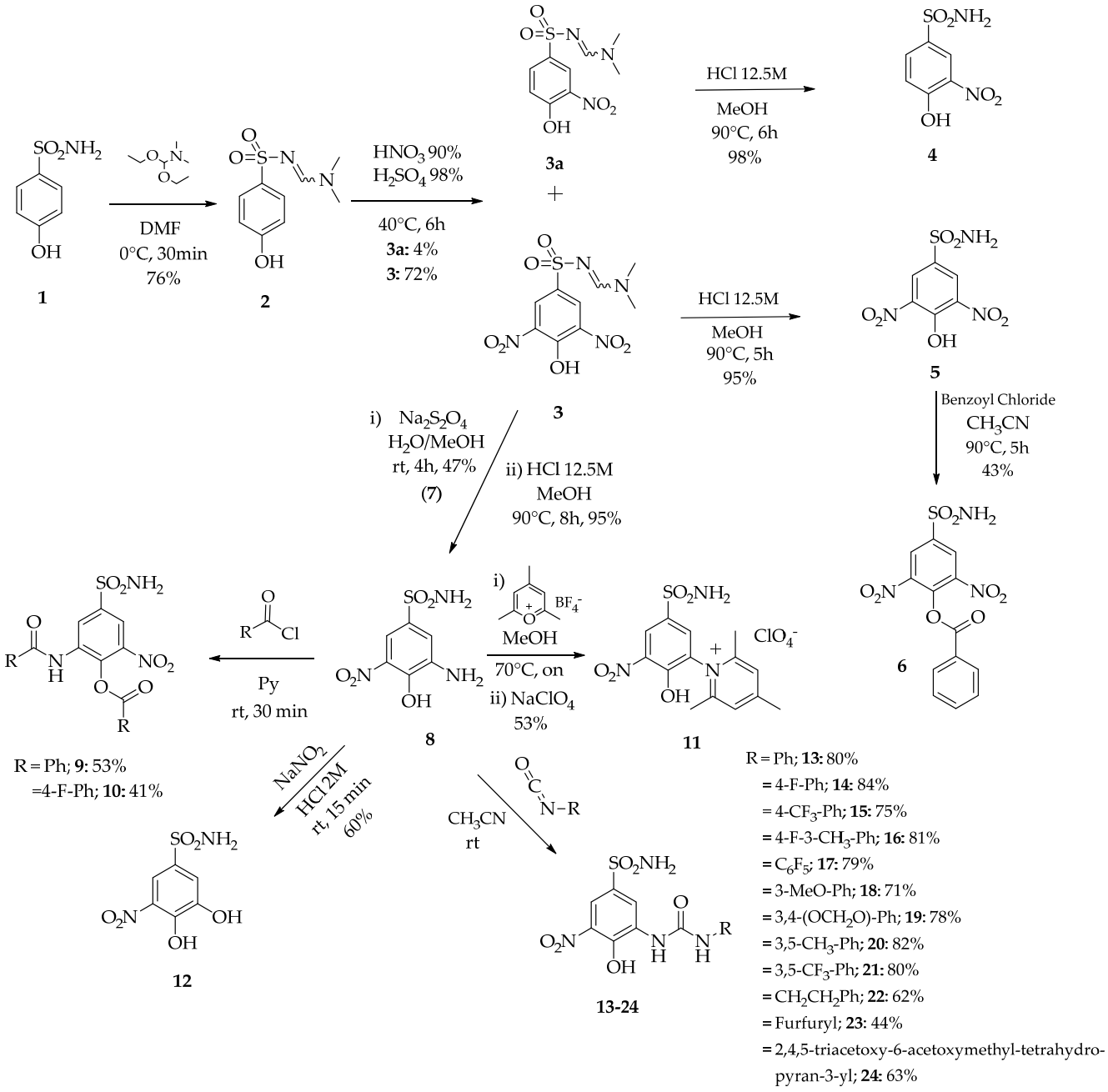

Scheme 2. General synthetic procedure of nitrobenzenesulfonamides **4-24**.

The main set of compounds, namely ureas **13-24,** were prepared by the reaction of **8** with commercially available isocyanates,[29] in addition to the freshly prepared one obtained from 1,3,4,6-tetra-*O*-acetyl-glucosamine.[48-49] Thereafter, compound **24** was de-acetylated with a sodium methoxide to give the glycoside **25** (Scheme 3)**.** All derivatives were characterized by ^{1}H-NMR, ^{19}F-NMR ^{13}C-NMR and mass spectrometry.

Of note, the set of ureido-derivatives feature peculiar spectroscopic properties. Indeed, it was not possible to observe any phenolic signal in the ^{1}H NMR of ureas **13-24** and their precursors **3, 7** and **8**. In addition, ureas **13-24** showed chromatic changes depending on the conditions to which they were subjected. Derivative **8,** which appears as a red solid, turned yellow after reaction with different isocyanates. The resulting yellow powder urea turned red again after purification by silica gel chromatography. MS was performed to confirm the derivatives identity was maintained. ^{1}H NMR signals of aromatic and exchangeable protons shifted to lower frequencies passing from the yellow to the red solid. Such a behavior could be related to intramolecular movement of electrons and intramolecular H-bond repositioning.

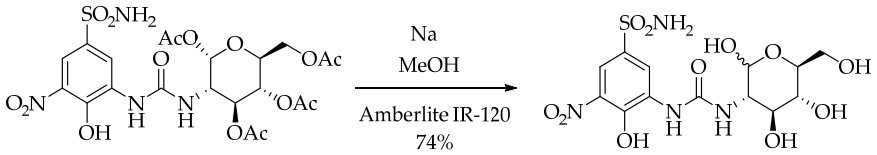

24 **25**

Scheme 3. Synthesis of derivative **25**.

Carbonic anhydrase inhibition

The CA inhibitory profiles of compounds **4-6** and **8-25** were evaluated by applying a stopped flow carbon dioxide hydrase assay,[50] in comparison to **AAZ** as standard CAI, against four physiologically significant isoforms CA I, II, IX and XII. The following SAR can be gathered from the inhibition data shown in Table 1:

Table 1. Inhibition data of CA isoforms CA I, II, IX and XII with sulfonamides **4-25** reported here and the standard sulfonamide inhibitor **AAZ** by a stopped flow CO_2 hydrase assay.[50]

	K_I (μM)			
Compound	CA I	CA II	CA IX	CA XII

4	0.91	0.24	0.12	0.16
5	4.35	0.18	0.10	0.08
6	4.79	0.84	0.09	0.07
8	6.18	0.61	0.21	0.20
9	1.38	0.39	0.13	0.30
10	2.90	0.46	0.10	0.21
11	>50	1.81	0.15	0.22
12	6.21	0.64	0.24	0.09
13	>50	2.78	0.94	0.83
14	5.39	0.53	0.34	0.50
15	5.20	0.20	0.63	0.95
16	7.58	0.21	0.37	0.88
17	0.69	0.27	0.29	0.08
18	8.20	5.15	0.46	0.53
19	>50	4.30	0.15	0.25
20	8.33	0.45	0.53	0.62
21	5.99	1.72	0.34	0.46
22	9.29	3.08	0.11	0.31
23	>50	2.53	0.39	0.53
24	5.67	1.90	0.29	0.79
25	4.92	0.86	0.17	0.16
AAZ	0.25	0.012	0.025	0.003

* Mean from 3 different assays, by a stopped flow technique (errors were in the range of ± 5% of the reported values).

(i) The cytosolic and off-target hCA I is the least inhibited isoform by sulfonamides **4-6**, **8-25** among those herein screened. Most derivatives act as low micromolar inhibitors, with K_Is spanning between 0.69 and 9.29 μM. The pyridium derivative **11** and urea derivative **19** and **23** did not inhibit CA I up to 50 μM. On the contrary, the pentafluorinated urea derivative **17** is the most efficient hCA I inhibitor with a K_I value of 0.69 μM. The simplest nitro compound **4** was also found to exhibit a sub-micromolar inhibitory efficiency. The remaining derivatives inhibit CA I in a rather narrow range that do not allow to compile further SAR.

(ii) Most nitro compounds inhibit the ubiquitous, off-target isoform CA II in a medium nanomolar to low micromolar range that spans from 0.18 to 5.15 μM. Among the non-ureido derivatives, the pyridinium **11** acts as micromolar CA II inhibitor with a K_I of 1.81μM. The substitution pattern of

the ureido moiety actively affects the CA II inhibition profiles within the urea subset. Incorporation of a methylene or ethylene spacer between the ureido-linker and the aromatic portion lowers the inhibitory efficiency of **22** and **23** (K_Is of 3.08 and 2.53 μM) with respect to compounds that bear a directly linked aromatic tail. Acetylation of the alcoholic groups on the glycosidic tail of **25** decreases the inhibition from 0.86 to 1.90 μM (**24**). Most evaluated substitution patterns at the ureidophenyl ring enhanced the enzymatic inhibition. Exceptions are compounds **18** and **19** that incorporate a 3-MeO or 3,4-(methylenedioxy) moiety, whose K_Is decreased from 2.78 (**13**) to 5.15 and 4.30 μM, respectively. The incorporation of fluorine atoms (**14**, **16**, **17**) or trifluoromethyl groups (**15**, **21**) on the benzene ring favoured CA II inhibition (K_Is of 0.20-0.53 μM) when compared to the unsubstituted **13**.

(iii) The tumor-associated isozymes CA IX and XII are the most efficiently inhibited by the reported nitro compounds, since all measured K_Is ranged between low to medium nanomolar range (0.10-0.94 μM). CA IX was found to be potently inhibited by all non-ureido derivatives, among which the di-nitrobenzoyl **6** exhibits a 95 nM K_I, representing the most active CA IX inhibitor herein reported. Likewise, its dinitro precursor **5** as well as the di-4-F-benzoylated nitro derivative **10** were measured to act as comparably potent inhibitors with K_Is of 0.10 μM. Again, the substitution pattern of the ureido moiety actively elicits the inhibitory trend spanning in the range 0.11-0.94 μM. The latter value belongs to derivative **13** that incorporates an unsubstituted, directly linked phenyl portion. The most favorable modifications in terms of CA IX inhibition include the separation of the phenyl ring from the urea by an ethylene spacer (**22**, K_I of 0.11 μM), the incorporation of a 3,4-(methylenedioxy) moiety at the benzene ring (**19**, K_I of 0.15 μM), or its replacement with a glycosidic portion (**25**, K_I of 0.17 μM). Acetylation of the alcoholic groups in the glycosidic tail lowers CA IX inhibition by 1.7-fold. Inclusion of a trifluoromethyl group at the *para* position of the phenyl moiety (**15**) was the least efficient substitution among those evaluated (K_I of 0.63 μM).

(iv) The target CA XII was potently inhibited by nitro derivatives **4-6** and **8-25**, with K_Is ranging between 0.08 and 0.95 μM. As for the previous isoform, non-ureido derivatives **4-6**, **8-12** generally afforded the most efficient inhibition. The presence of two nitro groups in **5** and its benzoylated derivatives **6** appeared to be favourable towards CA XII inhibition eliciting the lowest K_Is herein reported, 76 and 72 nM respectively. Of note, the catechol derivative **12** was also shwon to act as a strong CA XII inhibitor, with a K_I of 93 nM. CA XII features a region rich in Thr and Ser residues at the edge of the active site.[22] H-bonded interactions taking place between such residues and nitro and/or hydroxy moieties of **5**, **6** and **12** could ease the formation of the ligand-target adduct and likely justify the observed inhibition profiles. Ureido-derivatives **13-25** showed K_I inhibition values slightly higher and ranging between 0.08 and 0.95 μM when compared to compounds **4-12**. It is worth highlighting that the most efficient derivatives within this subset incorporate a pentafluorobenzene (**17**, K_I of 82 nM) and a glycosidic portion (**25**, K_I of 160 nM) on the ureido moiety. Accordingly, both portions were able to establish most of H-bonds contacts with the enzymatic counterpart. Conversely, other substitutions did not significantly affect the CA XII inhibition profile with respect to the unsubstituted, directly linked phenyl-bearing derivative **13** (K_I of 0.83). For instance, ureidophenyl compounds **15**, **16**, **20** and the O-acetylglycoside **24** inhibit CA XII in a comparable manner to **13** (K_Is in the range 0.79-0.95 μM). Remarkable inhibition is also shown by compound **16**, featuring the 3,4-(methylenedioxy) moiety at the benzene ring (K_I of 0.25 μM) and **22**, which incorporates an ethylene spacer between the urea and the aromatic tail (K_I of 0.31μM).

(v) The present inhibitory profiles differ by those previously reported for ureido-tailed benzenesulfonamides.[28-32] In fact, the data in Table 1 clearly report weaker inhibitions of all the considered isoforms. Though the nitro group at the *meta*-position of the benzene sulfonamide scaffold appears to be detrimental for CA inhibition, several derivatives maintain nanomolar efficacy and show interesting selective inhibition profiles depending on the substitution pattern.

The unsubstituted, directly linked phenyl-bearing derivative **13** exhibits a 3-fold selective action for CA IX/XII (K_Is of 0.94 and 0.83 μM) over CA II (K_I of 2.78 μM) and much greater over CA I (K_I > 50 μM). Fluorination of the ureido-aromatic portion reduces the selectivity of **14-17** for the tumor-associated isoforms by enhancing their CA I/II inhibitory potency (CA II: K_Is in the range 0.20-0.53 μM). As an exception, compound **21**, that bears a 3,5-di-CF_3-phenyl substituent showed an increased 5-fold CA IX/XII selectivity over II. Incorporation of methyl groups at the same positions of the aromatic ring increases the target promiscuity of derivative **20**. The selectivity for the tumor-associated isozymes also increased by appending 3-MeO (**18**) or 3,4-methylenedioxy (**19**) moieties at the aromatic portion, with the CA IX/II selectivity index (SI) of **19** reaching the value of 30. The detachment of the aromatic ring from the ureido linker by a methylene or ethylene spacer enhances again the preferential efficacy of **22** and **23** for CA IX and XII by 10-fold when the SI are compared to those of derivative **13**. The acetylation of the glycoside alcoholic groups of **25** markedly enhanced the inhibition of the tumor-associated isoforms in comparison to hCA II.

X-ray crystallography

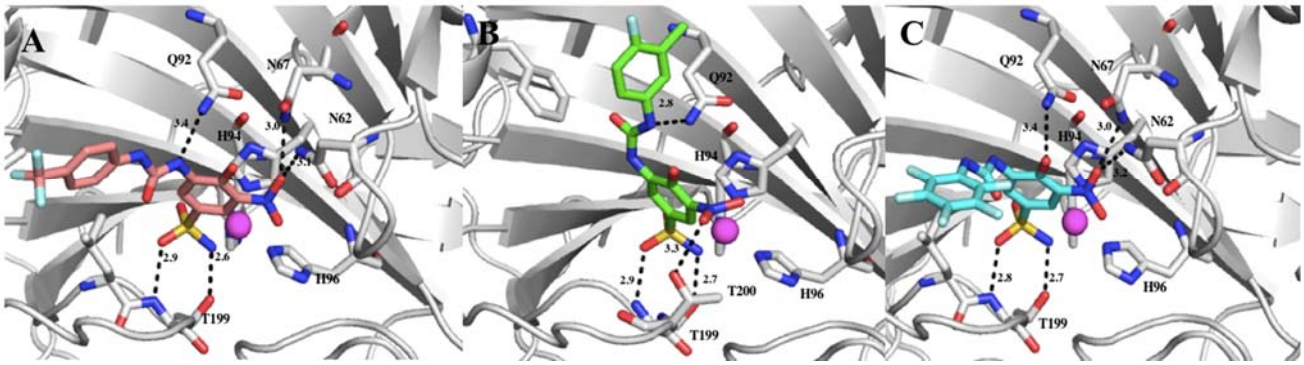

Figure 3. Crystal structures of CA II (gray) in complex with inhibitors **A) 15** (pink), **B) 16** (green) and **C) 17** (cyan). Hydrogen bonds (2.5 - 3.5 Å) are depicted as black dotted lines. The zinc is shown as a magenta sphere.

The X-ray crystal structures of CA II and CA IX/mimic were determined in complex with inhibitors **15**, **16** and **17** (Figures 3 and 4). All six datasets had overall redundancies in the range of 2.4-3.9 with completeness above 90% (Table 1). Of note, the R_{pim} values were consistently higher in the CA II structures in comparison to the CA IX/mimic structures. Also, the resolution was consistently higher in the CA IX/mimic structures. The quality of resulting electron density for the compounds were similar in CA II and CA IX/mimic (Supplementary Figure S1). Interestingly, a single inhibitor molecule was bound in the active site of each CA II structure (Site I) whereas additional inhibitors (Sites II and III) were observed to bind around the CA IX/mimic active site (Supplementary Figure S2).

All three inhibitors (Site I) were observed to bind directly to the active site zinc through the N1 atom of the sulfonamide group (~2.0 Å), displacing the catalytic zinc-bound solvent (Figures 3 and 4). As previously observed in similar CA sulfonamide complexes, additional hydrogen bonds from T199 N and OG to the sulfonamide oxygen atoms were present. An unusual orientation of the benzene ring was observed with respect to most of the previously observed CA-benzenesulfonamide adducts. (Supplementary Figure S3). Indeed, the presence of the nitro group in position 3 of the scaffold elicits a torsion to the ligand that enables conservation of the coordination, but impairs hydrophobic and π-π interactions with the aromatic residues nearby. The nitro group protrudes toward H64, forming H-bonds with residues in the hydrophilic side of the cavity. Such a deviation from the usual aromatic ring position can justify the generally reduced CA inhibition profiles reported in Table 1 when compared to previously reported ureido-substituted benzenesulfonamides, such as **SLC-0111**.

The orientation of the tails extending out of the active site differed between the three compounds (Figures 3 and 4). In CA II, inhibitors **15** and **17** were observed to bind in the hydrophobic region, whereas **16** oriented toward the interface of the hydrophobic and hydrophilic regions of the active site. Conversely, inhibitors **17** and **16** bound in the hydrophobic region and **15**

was bound at the hydrophobic/hydrophilic interface of CA IX/mimic (Figure 4A-C). Multiple inhibitors of **15** and **17** were bound in the CA IX/mimic active site (Supplementary Figure S2).

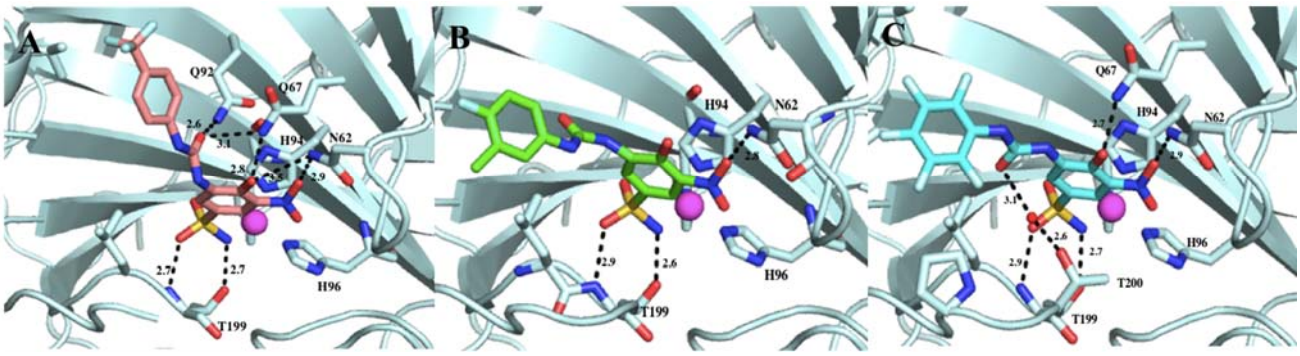

Figure 4. Crystal structures of CA IX/mimic (cyan) in complex with inhibitors **A) 15** (pink), **B) 16** (green) and **C) 17** (cyan). Hydrogen bonds (2.5 - 3.5 Å) are depicted as black dotted lines. The zinc and solvent are shown as magenta and red spheres, respectively.

For inhibitor **15** bound in CA II (site I), additional hydrogen bonds were observed between Q92 and the amine group of the linker (3.4 Å), and between N67 and N62 and the nitro oxygen of the inhibitor (3.0 and 3.1 Å, respectively). In CA IX/mimic, hydrogen bonds existed between Q67 and Q92 and the carboxyl group of the linker (3.3 and 2.6 Å, respectively), Q67 and the hydroxyl group of inhibitor (2.8 Å), and N62 and the hydroxyl and oxygen of NO_2 (3.5 and 2.9 Å, respectively). Additional van der Waal interactions with residues F131, V135, and L198 in CA II and S65, V131 and L198 in CA IX/mimic further stabilize the tail of the compound (Fig 4A-B). The surface area covered by **15** was 326 Å in CA II and 296 Å in CA IX/mimic. Fewer van der Waals interactions are expected in CA IX/mimic due to the smaller inhibitor-bound surface area, likely caused by the F131V variation, contributing to the 3-fold selectivity of **15** for CA II over CA IX (Table 1).

For inhibitor **17** bound in CA II (site I), hydrogen bond interactions were observed between Q92 and the hydroxyl group of the inhibitor (3.4 Å), N67 and N62 and the nitro oxygen of the

inhibitor (3.5 and 3.2 Å, respectively). In CA IX/mimic, interactions existed between Q67 and the inhibitor hydroxyl group (2.7 Å) and N62 and nitro oxygen of the inhibitor (2.9 Å). Van der Waal interactions were observed between the inhibitor and L198 in CA II and V131, V135, L198 and P202 in CA IX/mimic (Fig 4C-D). The tail was observed to flip approximately 90° in CA II to accommodate the steric hindrance by F131. The surface area covered by the ligand in the active site of CA II was 353 $Å^2$ and 330 $Å^2$ in CA IX/mimic. The increased number of van der Waals interactions observed in CA IX/mimic were balanced by the greater number of hydrogen bonds in CA II, suggesting the similar affinities of **17** for both CA II and CA IX/mimic (Table 1).

For inhibitor **16** bound in CA II (site I), hydrogen bond exists between Q92 and the amine group of the linker (2.8 Å) and T200 and nitro oxygen of the inhibitor (3.3 Å). In CA IX/mimic, these interactions were observed between N62 and nitro oxygen of **16** (2.8 Å). Van der Waal interactions existed between **16** and Q69, F131 and L198 in CA II and L198 in CA IX/mimic. The surface area covered by **16** was 373 $Å^2$ and 358 $Å^2$ in CA II and CA IX/mimic, respectively. The greater number of van der Waals interactions and hydrogen bonds observed in CA II support the 2-fold selectivity of **16** for CA II over CA IX/mimic (Table 1).

Table 2: Crystallographic statistics

	CA II			CA IX/mimic		
	15	**16**	**17**	**15**	**16**	**17**
PDB code	6EBE	6EDA	6ECZ	6EEA	6EEO	6EEH
Space group	$P2_1$					
Cell dimensions (Å, °)	42.86 41.81 72.91 104.6	42.89 41.93 72.87 104.5	42.88 41.88 72.91 104.5	42.59 41.889 72.79 104.1	42.59 41.94 72.76 104.1	42.57 41.80 72.89 104.1
Resolution (Å)	32.39-1.88	19.08-1.99	29.5-2.21	29.42-1.64	18.97-1.72	29.38-1.63
Total reflections	18182	16556	12377	29121	26482	28938
I/Iσ	6.2	1.93	1.95	2.31	2.0	1.5

Redundancy	2.4	3.1	3.8	3.0	3.9	2.7
Completeness (%)	90.4	95.9	94.5	92.8	100	93.6
Rpim (%)	6.9	7.3	8.5	4.3	3.5	4.5
Rcryst (%)	22.2	26.5	20.7	23.4	23.0	28.6
Rfree (%)	29.5	35.6	26.7	23.0	26.7	31.3
# of Protein Atoms	2049	2055	2049	2042	2079	2042
# of Water molecules	48	32	18	62	26	81
# of Ligand atoms	28	26	29	56	37	87
Ramachandran stats (%): Favored, allowed.	95.7, 4.3	96.5, 3.5	95.2, 4.8	96.8, 3.2	97.7, 2.3	97.6, 2.4
Avg. B factors ($Å^2$): Main-, side-chain, ligand(s) I, II, III	19.9, 27.4, 47.5 (I)	19.4, 25.9, 45.5 (I)	33, 39.3, 73.2 (II)	14.8, 21.7, 35.8 (I), 80.86 (II)	20.6, 27.5, 47.7 (I)	15.9, 23.2, 28.3 (I), 60.9 (II), 43.6 (III).
rmsd for bond lengths, angles (Å, º)	0.009, 1.295	0.011, 1.584	0.009, 1.408	0.007, 1.458	0.009, 1.596	0.007, 1.234

R_{pim}- the precision of the averaged intensity measurements which gives the standard error of the mean.

R_{sym}- measure of agreement among the independent measurements of symmetry-related reflections in a crystallographic data set.

R_{cryst}- measures the agreement between the model and the observed data.

Cytotoxicity Assay

Several compounds that exhibited the best inhibitory profiles within the ureas series (**14**, **17**, **19**, **21**, **22**, **24**) and the non-ureido subset (**5**, **8**, **10**, **11**) were chosen (30-200 μM) to evaluate their effects on the viability of human colon cancer HT-29 cells, breast adenocarcinoma MDA-MB-231 cells and prostatic cancer PC-3 cells via MTT assay. The efficacy of the compounds over 48h is summarized in Figure 6 (and Table S1-3 in ESI). The untreated control showed 100% viability. The effect of **SLC-0111** on viability of the three cell lines is also reported (Table S4 in ESI).

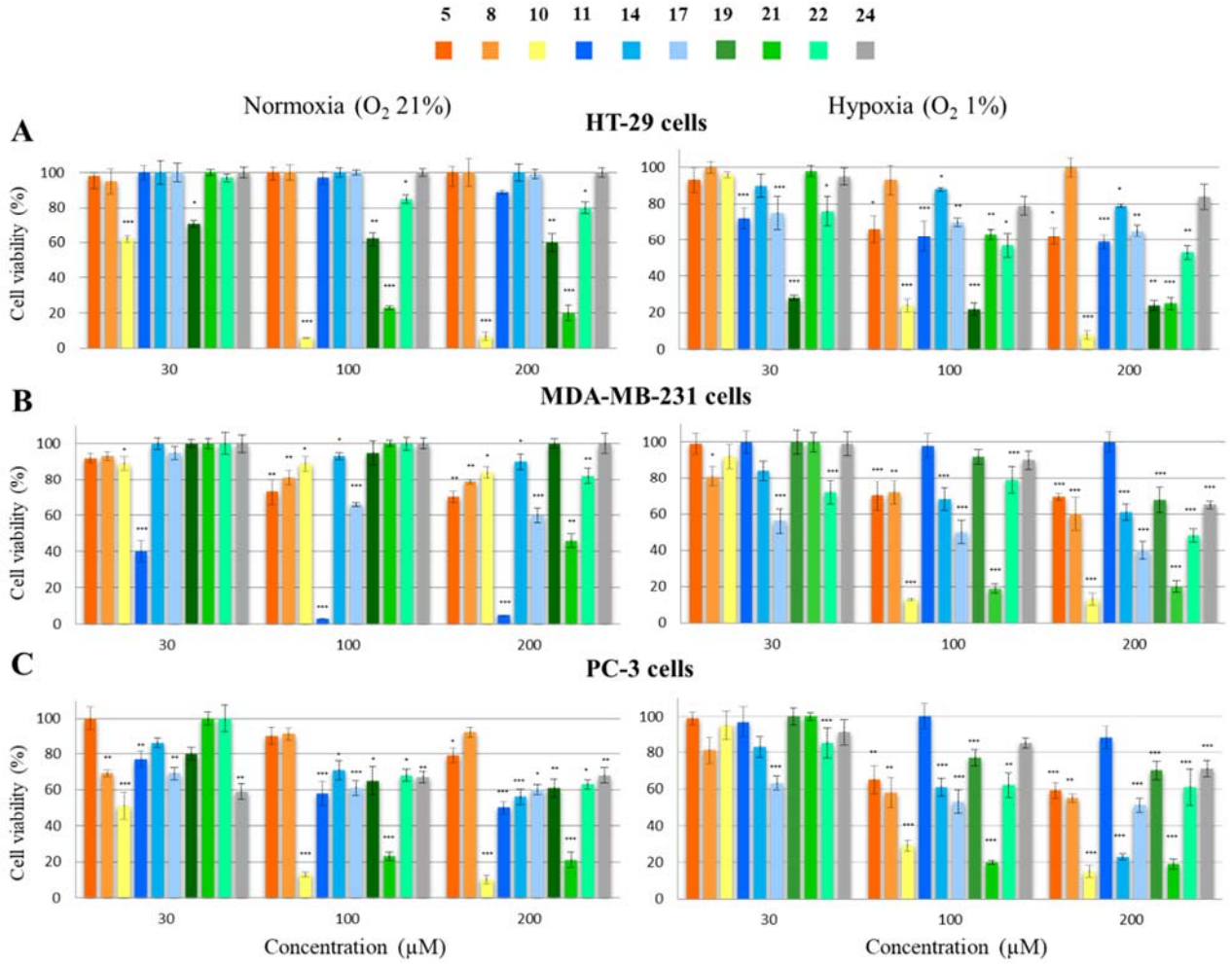

Figure 6. (A) HT-29, (B) MDA-MB-231, (C) PC-3 cells ($1x10^4$/well) were treated with compounds **5**, **8**, **10**, **11**, **14**, **17**, **19**, **21**, **22**, **24** (30 - 200 μM). Incubation was allowed for 48 h in normoxic (20% O_2) and hypoxic conditions (1% O_2). Control condition was arbitrarily set as 100% and values are expressed as the mean ± S.E.M. of three experiments. *P<0.05, **P<0.01 and ***P<0.001 in comparison to control (0 μM, not shown).

The greatest anti-proliferative action was displayed after an incubation of 48h. Short incubation time (16h) with the compounds were tested for HT-29 cell lines and are reported in ESI (Figure S4). Although partially, hypoxia enhanced the efficacy of many of the screened compounds in reducing cancer cell viability depending on the concentration and type of cell line. It is worth stressing that other CAIs, such as such as sulfocoumarins,[51] 3-hydroxyquinazoline-2,4-diones,[31] selenoureido-benzensulfonamides,[52] chromeno[4,3-c]pyrazol-4-ones [53] and nitrogenous base-bearing benzenesulfonamides [54] did not show hypoxia-enhanced anti-proliferative efficacy *in vitro,*

although they exhibited potent inhibitory action against the hypoxia-induced CA IX and CA XII. It could be speculated that the brief time that cells spend in low oxygen conditions does not produce sufficient CA IX/XII overexpression with respect to cells treated in normoxic conditions. However, this evidence validates the herein reported data. As a result, the increase of cytotoxicity of nitrobenzenesulfonamides in hypoxic conditions likely shows the introduction of alternative mechanism of action, such as prodrugs activation.

In detail, of the ten assayed nitro-aromatics, six compounds exhibited hypoxia-increased cytotoxic effects against HT-29 cells, eight against MDA-MB-231 cells, and four against PC-3 cells in a concentration-dependent manner (Figure 6, Table S1-3 in ESI). Among the non-ureido derivatives, the di-(4-F-benzoyl) derivative **10** was the best anti-proliferative agent, reducing the number of living cells up to 6% in HT-29, 13% in MDA-MB-231 and 8% in PC-3 cell lines. Whereas this strong effect resulted not to be related to hypoxia in HT-29 and PC-3 cells, a strong hypoxic activation arose with breast cancer cells. Interestingly, the pyridinium salt **11** showed a better *in vitro* efficacy in normoxic conditions with PC-3 cells and mostly with MDA-MB-231 ones, reducing the viability of the culture up to 40% at 30 μM and 3% at 100 μM. These results are in agreement with the behavior of pyridinium-bearing benzenesulfonamides, whose permanent positive charge does not allow sufficient crossing of the membrane. Precursors **5** and **8** do not shown remarkable effects.

The di-3,5-CF_3-phenyl derivative **21** exhibits the best anti-proliferative profile among the tested ureas. Its efficacy against MDA-MB-231 cell is 4-fold enhanced by hypoxia at 100 μM, whereas it is equal in normoxic and hypoxic conditions for HT-29 and PC-3 cells. The 3,4-(methylenedioxy)phenylurea **19** proved to be more active against HT-29 in hypoxic conditions in comparison to normoxic. Most remaining ureido compounds demonstrated weak to medium cytotoxic effects increased by hypoxia. The hypothesis of bio-reductive pathways undergone by the nitrobenzenesulfonamides is partially supported by the reported data. Literature data would suggest that hydroxilamine and nitroso derivatives are the most likely produced cytotoxic species.

Nevertheless, further studies are currently ongoing to properly typify the nature of the cytotoxins as well as the activation mechanisms taking place in hypoxic conditions.

Conclusions

Hypoxia promotes a multitude of effects on tumor biology. Overexpression of CA IX and CA XII aids the tumor cells to maintain a suitable intra/extracellular pH for cancer cell survival and growth. Hypoxia also furthers the activity of specific one-electron and two-electron oxido-reductases, that may be exploited to achieve a selective bio-reductive prodrugs activation to cytotoxin. Herein, we designed new selective CA IX/XII inhibitors, as analogues of the anti-tumor phase II entering drug **SLC-0111**. Derivatives of the ureido-benzenesulfonamide-type were appended with a nitro-aromatic moiety to yield an anti-proliferative action increased by hypoxia. Several such derivatives display nanomolar efficacy and show interesting CA IX/XII selective inhibition profiles over the off-target CA I/II. X-ray crystallography of the adduct of three inhibitors with both CA II and IX/mimic rationalized the compounds generally worsened inhibitory profiles with respect to previously reported ureido-benzenesulfonamides. The effects of some selected compounds on the viability of human colorectal HT-29, breast adenocarcinoma MDA-MB-231, prostate PC-3 cancer cell lines have been evaluated in both normoxic and hypoxic conditions. It can be noted that hypoxia has a low to medium effect on the efficacy of many screened compounds in reducing cancer cells viability depending on the concentration and type of cell line. Since other CAIs, such as such as AAZ, SLC-0111, sulfocoumarins,[51] 3-hydroxyquinazoline-2,4-diones,[31] selenoureido-benzensulfonamides,[52] chromeno[4,3-c]pyrazol-4-ones[53] and nitrogenous base-bearing benzenesulfonamides [54] did not show hypoxia-enhanced anti-proliferative efficacy *in vitro* in spite of a potent inhibitory action against the hypoxia-induced CA IX and CA XII, the herein reported data support evidence of a hypoxia-strengthened cytotoxic action by nitrobenzenesulfonamides. The present study provided the initiation towards the development of hypoxia-activated anti-tumor CAIs. Further experiments are currently ongoing to prove that a bioreduction process is taking

place. New nitro-derivatives have been designed which incorporate the tail in *para* position of the benzenesulfonamide scaffold to overcome the steric hindrance of the nitro moiety and yield a greater CA IX/XII inhibition and as a result, more marked *in vitro* cytotoxicity.

Experimental protocols

Chemistry

Anhydrous solvents and all reagents were purchased from Sigma-Aldrich, Fluorochem and TCI. All reactions involving air- or moisture-sensitive compounds were performed under a nitrogen atmosphere using dried glassware and syringes techniques to transfer solutions. Nuclear magnetic resonance (^{1}H-NMR, ^{19}F-NMR, ^{13}C-NMR) spectra were recorded using a Bruker Advance III 400 MHz spectrometer in DMSO-d_6. Chemical shifts are reported in parts per million (ppm) and the coupling constants (J) are expressed in Hertz (Hz). Splitting patterns are designated as follows: s, singlet; d, doublet; sept, septet; t, triplet; q, quartet; m, multiplet; brs, broad singlet; dd, doublet of doublets. The assignment of exchangeable protons (OH and NH) was confirmed by the addition of D_2O. Analytical thin-layer chromatography (TLC) was carried out on Sigma silica gel F-254 plates. Flash chromatography purifications were performed on Sigma Silica gel 60 (230-400 mesh ASTM) as the stationary phase and MeOH/DCM were used as eluents. Melting points (mp) were measured in open capillary tubes with a Gallenkamp MPD350.BM3.5 apparatus and are uncorrected.

The HPLC analysis was performed by using an Agilent 1200 Series equipped by autosampler, binary pump system and diode array detector (DAD). The column used was a Luna PFP 30 mm length, 2 mm internal diameter and 3 μm particle size (Phenomenex, Bologna, Italy) at constant flow of 0.25 mL min^{-1}, employing a binary mobile phase elution gradient. The solvents used were 10 mM formic acid and 5 mM ammonium formate in mQ water solution (solvent A) and 10 mM formic acid and 5 mM ammonium formate in methanol (solvent B) according to the elution gradient as follow: initial at 90% solvent A, which was then decreased to 10% in 8 min, kept for 3 min,

returned to initial conditions in 0.1 min and maintained for 3 min for reconditioning, to a total run time of 14 min. The stock solution of each analyte was prepared in methanol at 1.0 mg mL^{-1} and stored at 4 °C. The sample solution of the analyte was freshly prepared by diluting its stock solution up to a concentration of 10 μg mL^{-1} in mixture of mQ water:methanol 50:50 (v/v) and 5 μL were injected in the HPLC system. The chromatographic profiles of each analyte (ESI p. S24) were monitored at 230 nm, that represents the maximum UV absorption for these compounds. All compounds reported were >95% HPLC pure. The solvents used in HPLC measures were methanol (Chromasolv grade), purchased from Sigma-Aldrich (Milan - Italy), and mQ water 18 MΩ, obtained from Millipore's Simplicity system (Milan-Italy). High resolution mass spectrometry (HR-MS) analysis were performed with a Thermo Finnigan LTQ Orbitrap mass spectrometer equipped with an electrospray ionization source (ESI). Analysis were carried out in negative ion mode monitoring the $[M-H]^-$ species, and it was used a proper dwell time acquisition to achieve 60,000 units of resolution at Full Width at Half Maximum (FWHM). Elemental composition of compounds were calculated on the basis of their measured accurate masses, accepting only results with an attribution error less than 5 ppm and a not integer RDB (double bond/ring equivalents) value, in order to consider only the protonated species.[55] None of the screened derivatives reported PAINS alerts determined by SwissADME server (www.swissadme.ch).

N,N-dimethylaminomethylene-4-hydroxy-benzenesulfonamide (2).[56]

N,N-Dimethylformamide dimethyl acetal (1.2 eq) was added to a solution of compound 4-hydroxybenzenesulfonamide **1** (2.0 g, 1.0 eq) in DMF (1.5 ml) at 0°C and that was stirred at r.t. for 0.25h. The reaction mixture was quenched with EtOAc (40 ml) and the formed precipitate was filtered and purified by silica gel column chromatography eluting with MeOH/DCM 5% to afford compound **2** as a yellow solid. 76% yield; silica gel TLC R_f 0.22 (MeOH/DCM 5 % *v/v*); δ_H (400 MHz, DMSO-d_6): 2.92 (s, 3H, CH_3), 3.16 (s, 3H, CH_3), 6.88 (d, J = 8.4. 2H), 7.61 (d, J = 8.4. 2H),

8.18 (s, 1H), 10.29 (bs, 1H, exchange with D_2O, O*H*); δ_C (100 MHz, DMSO-d_6): 35.9, 41.7, 116.2, 129.1, 134.2, 160.3, 161.3.

N,N-dimethylaminomethylene-4-hydroxy-3,5-dinitro-benzenesulfonamide (3) and N,N-dimethylaminomethylene-4-hydroxy-3-nitro-benzenesulfonamide (3a).

N,N-Dimethylaminomethylene-4-hydroxy-benzenesulfonamide (1.0 g, 1.0 eq) was added portion wise to a mixture of concentrated H_2SO_4 (2.2 mL) and fuming HNO_3 (1.6 mL) at 0°C and the obtained solution was stirred at 40°C for 4h. The reaction mixture was cooled and quenched with slush (40 ml) and the formed precipitate was filtered-off, dried under *vacuo* and purified by silica gel column chromatography eluting with MeOH/EtOAc from 5 to 10% to afford the titled compounds **3** and **3a** as yellow solids. **(3)** 72% yield; m.p. >300°C; silica gel TLC R_f 0.46 (MeOH/DCM 20 % *v/v*); δ_H (400 MHz, DMSO-d_6): 2.95 (s, 3H, C*H*$_3$), 3.17 (s, 3H, C*H*$_3$), 8.22 (s, 1H), 8.29 (s, 2H); δ_C (100 MHz, DMSO-d_6): 36.1, 42.0, 128.1, 128.5, 141.8, 152.9, 161.1.

(3a) 4% yield; m.p. 195-198°C; silica gel TLC R_f 0.60 (MeOH/DCM 5 % *v/v*); δ_H (400 MHz, DMSO-d_6): 2.95 (s, 3H, C*H*$_3$), 3.18 (s, 3H, C*H*$_3$), 7.27 (d, *J* = 8.6, 1H), 7.92 (dd, *J* = 2.4, 8.6, 1H), 8.24 (d, *J* = 2.4, 1H), 8.24 (s, 1H), 11.94 (bs, 1H, exchange with D_2O, O*H*); δ_C (100 MHz, DMSO-d_6): 36.1, 41.9, 120.7, 124.4, 133.2, 134.6, 137.3, 155.4, 160.9.

4-Hydroxy-3-nitro-benzenesulfonamide (4).

A suspension of N,N-dimethylaminomethylene-4-hydroxy-3-nitro-benzenesulfonamide **3a** (0.04 g, 1.0 eq) in MeOH (3 ml) was treated with HCl 12M (0.5 ml) and stirred at 90°C for 6h. The reaction mixture was concentrated in *vacuo*, treated with H_2O (5 ml) and extracted with EtOAc (3x10 ml). The combined organic layers were dried over Na_2SO_4, filtered-off and concentrated in *vacuo* to give the titled compound **4.** 98% yield; m.p. 201-203°C; silica gel TLC R_f *0.26* (MeOH/DCM 5 % *v/v*); δ_H (400 MHz, DMSO-d_6): 7.31 (d, *J* = 8.6, 1H), 7.47 (s, 2H, exchange with D_2O, SO_2NH_2), 7.96 (dd, *J* = 2.4, 8.6, 1H), 8.32 (d, *J* = 2.4, 1H), 12.01 (bs, 1H, exchange with D_2O, O*H*); δ_C (100 MHz,

DMSO-*d*$_6$): 120.8, 124.4, 132.9, 135.5, 137.1, 155.7; ESI-HRMS (m/z) [M-H]$^-$: calculated for $C_6H_5N_2O_5S$ 216.9914; found 216.9917.

4-Hydroxy-3,5-dinitro-benzenesulfonamide (5).

A suspension of N,N-dimethylaminomethylene-4-hydroxy-3,5-dinitro-benzenesulfonamide **3** (0.8 g, 1.0 eq) in MeOH (20 ml) was treated with HCl 12M (4 ml) and stirred at 90°C for 5h. The reaction mixture was concentrated in *vacuo*, treated with H_2O (20 ml) and extracted with EtOAc (3x20 ml). The combined organic layers were dried over Na_2SO_4, filtered-off and concentrated under *vacuo* to give a residue that was purified by silica gel column chromatography eluting with MeOH/DCM 10% to afford the titled compound **5** as a yellow solid**.** 95% yield; m.p. >300°C; silica gel TLC R_f 0.23 (MeOH/DCM 20 % *v/v*); δ_H (400 MHz, DMSO-*d*$_6$): 7.14 (s, 2H, exchange with D_2O, SO_2NH_2), 8.19 (s, 2H); δ_C (100 MHz, DMSO-*d*$_6$): 118.6, 128.8, 143.2, 160.7; ESI-HRMS (m/z) [M-H]$^-$: calculated for $C_6H_4N_3O_7S$ 261.9765; found 261.9760.

Benzoic acid 2,6-dinitro-4-sulfamoyl-phenyl ester (6).

Benzoyl chloride (1.5 eq) was added dropwise to a solution of 4-hydroxy-3,5-dinitro-benzenesulfonamide **5** (0.1 g, 1.0 eq) in CH_3CN (4 ml) under a nitrogen atmosphere and that was stirred at 90°C for 5h. The reaction mixture was concentrated in *vacuo* and the obtained residue was purified by silica gel column chromatography eluting with EtOAc/Hexane 60% to afford the titled compound **6** as a white solid. 43% yield; m.p. 202-203°C; silica gel TLC R_f 0.28 (EtOAc/n-hexane 40 % *v/v*); δ_H (400 MHz, MeO*D-d4*): 7.63 (t, *J* = 7.8, 2H), 7.79 (t, *J* = 7.8, 1H), 8.18 (d, *J* = 7.8, 2H), 8.89 (s, 2H); δ_C (100 MHz, MeO*D-d4*): 127.5, 127.8, 129.3, 130.9, 135.3, 140.9, 143.9, 144.3, 163.3; ESI-HRMS (m/z) [M-H]$^-$: calculated for $C_{13}H_8N_3O_8S$ 366.0027; found 366.0029.

N'-((3-Amino-4-hydroxy-5-nitrophenyl)sulfonyl)-N,N-dimethylformimidamide (7).

Sodium hydrosulfite (3.0 eq) was added portion wise to a suspension of N,N-dimethylaminomethylene-4-hydroxy-3,5-dinitro-benzenesulfonamide **3** (0.5g, 1.0 eq) in H_2O/MeOH ¼ (12 ml). The reaction mixture was stirred at r.t. for 4h, quenched with HCl 0.5M (25 ml) and extracted with EtOAc (3x30 ml). The organic layers were dried over Na_2SO_4, filtered-off and concentrated under *vacuo* to give a residue that was purified by silica gel column chromatography eluting with MeOH/DCM 3% to afford the titled compound **7** as a red solid. 47% yield; m.p. 222-225°C; silica gel TLC R_f 0.32 (MeOH/DCM 10 % *v/v*);δ_H (400 MHz, DMSO-d_6): 2.95 (s, 3H, CH_3), 3.18 (s, 3H, CH_3), 7.29 (d, J = 8.4, 1H), 7.40 (bs, 2H, exchange with D_2O, NH_2, overlap with signal at 7.29 and 7.50), 7.50 (dd, J = 2.4, 8.8, 1H), 8.19 (s, 1H); δ_C (100 MHz, DMSO-d_6): 36.0, 41.8, 109.6, 114.9, 135.1, 135.6, 141.94, 143.4, 160.5; ESI-HRMS (m/z) $[M-H]^-$: calculated for $C_9H_{11}N_4O_5S$ 287.0445; found 287.0448.

3-Amino-4-hydroxy-5-nitro-benzenesulfonamide (8).

A suspension of 3-amino-N,N-dimethylaminomethylene-4-hydroxy-5-nitro-benzenesulfonamide **7** (0.4 g, 1.0 eq) in MeOH (10 ml) was treated with HCl 12M (2 ml) and stirred at 90°C for 8h. The reaction mixture was concentrated in *vacuo*, treated with H_2O (20 ml) and extracted with EtOAc (3x20 ml). The combined organic layers were dried over Na_2SO_4, filtered-off and concentrated under *vacuo* to give a residue that was purified by silica gel column chromatography eluting with MeOH/DCM 10% to afford compound **8** as a red solid**.** 95% yield; m.p. 232-234°C; silica gel TLC R_f 0.11 (MeOH/DCM 5 % *v/v*); δ_H (400 MHz, DMSO-d_6): 7.30 (d, J = 1.8, 1H), 7.34 (s, 2H, exchange with D_2O, SO_2NH_2) 7.60 (dd, J = 1.8, 1H); δ_C (100 MHz, DMSO-d_6): 109.7, 114.0, 135.4, 135.6 142.2, 144.3; ESI-HRMS (m/z) $[M-H]^-$: calculated for $C_6H_6N_3O_5S$ 232.0023; found 232.0026.

General synthetic procedure of benzoic acid 2-benzoylamino-6-nitro-4-sulfamoyl-phenyl esters 9-10.

The proper benzoyl chloride (1.5 eq) was added dropwise to a solution of 3-amino-4-hydroxy-5-nitro-benzenesulfonamide **8** (0.06 g, 1.0 eq) in dry pyridine (1.5 ml) under a nitrogen atmosphere and that was stirred at r.t. for 0.5h. The reaction mixture was quenched with 1M HCl (10 ml) and extracted with EtOAc (2x15 ml) The organic layers were dried over Na_2SO_4, filtered-off and concentrated under *vacuo* to give a residue that was purified by silica gel column chromatography eluting with EtOAc/*n*-hexane 50% to afford the titled compounds **9-10**.

Benzoic acid 2-benzoylamino-6-nitro-4-sulfamoyl-phenyl ester (9).

Benzoic acid 2-benzoylamino-6-nitro-4-sulfamoyl-phenyl ester **9** was obtained according the general procedure earlier reported using 3-amino-4-hydroxy-5-nitro-benzenesulfonamide **8** (0.06 g, 1.0 eq) and benzoyl chloride (1.5 eq) in dry pyridine. 53% yield; m.p. 216-217°C; silica gel TLC R_f 0.72 (MeOH/DCM 20 % *v/v*); δ_H (400 MHz, DMSO-d_6): 7.53 (t, J = 7.2, 2H), 7.63 (m, 3H), 7.81 (t, J = 7.2, 1H), 7.86 (s, 2H, exchange with D_2O, SO_2NH_2), 7.90 (d, J = 7.2, 2H), 8.17 (d, J = 7.2, 2H), 8.46 (d, J = 2.4, 1H), 8.66 (d, J = 2.4, 1H), 10.71 (s, 1H, exchange with D_2O, N*H*CO); δ_C (100 MHz, DMSO-d_6): 120.2, 128.7, 128.8, 128.9, 129.5, 130.1, 131.1, 133.2, 134.4, 134.9, 135.8, 139.8, 142.9, 143.5, 163.7, 167.12; ESI-HRMS (m/z) $[M-H]^-$: calculated for $C_{20}H_{14}N_3O_7S$ 440.0547; found 440.0540.

4-F-Benzoic acid 2-(4-F-benzoyl)amino-6-nitro-4-sulfamoyl-phenyl ester (10).

4-F-Benzoic acid 2-(4-F-benzoyl)amino-6-nitro-4-sulfamoyl-phenyl ester **10** was obtained according the general procedure earlier reported using 3-amino-4-hydroxy-5-nitro-benzenesulfonamide **8** (0.06 g, 1.0 eq) and 4-F-benzoyl chloride (1.5 eq) in dry pyridine. 41% yield; m.p. 217-220°C; silica gel TLC R_f (EtOAc/n-hexane 50 % *v/v*); δ_H (400 MHz, DMSO-d_6): 7.39 (t, J = 8.8, 2H), 7.48 (t, J = 8.8, 2H), 7.86 (s, 2H, exchange with D_2O, SO_2NH_2), 7.98 (m, 2H), 8.25 (m, 2H), 8.46 (d, J = 2.4, 1H), 8.66 (d, J = 2.4, 1H), 10.72 (s, 1H, exchange with D_2O, N*H*CO); δ_F (376 MHz, DMSO-d_6): -107.47 (s, 1F), -103.07 (s, 1F);δ_C (100 MHz, DMSO-d_6): 116.6 (d, J^2CF = 22.0),

117.4 (d, J^2CF = 22.2), 120.3, 125.3, 129.0, 130.8, 131.6 (d, J^3CF = 9.2), 134.2 (d, J^3CF = 9.9), 134.8, 139.7, 142.9, 143.4, 162.8, 165.4 (d, J^1CF = 248.8), 166.1, 166.9 (d, J^1CF = 252.3); ESI-HRMS (m/z) $[M-H]^-$: calculated for $C_{20}H_{12}F_2N_3O_7S$ 476.0359; found 476.0362.

1-(2-Hydroxy-3-nitro-5-sulfamoyl-phenyl)-2,4,6-trimethyl-pyridinium, perchlorate salt (11).

2,4,6-Trimethyl-pyrylium, tetrafluoroborate salt (1.2 eq) was added to a solution of 3-amino-4-hydroxy-5-nitro-benzenesulfonamide **8** (0.06 g, 1.0 eq) in dry MeOH (4 ml) under a nitrogen atmosphere and that was stirred at 70°C overnight. The reaction mixture was quenched with H_2O (10 ml) and treated with 1M $NaClO_4$ aqueous solution (3 eq). The formed precipitate was filtered and purified by silica gel column chromatography eluting with MeOH/DCM 15% to afford the titled compounds **11.** 53% yield; m.p. 230°C dec.; silica gel TLC R_f 0.05 (MeOH/DCM 10 % *v/v*); δ_H (400 MHz, DMSO-d_6): 2.39 (s, 6H, 2 x CH_3), 2.61 (s, 3H, CH_3), 7.10 (s, 2H, exchange with D_2O, SO_2NH_2), 7.83 (d, *J* = 2.4, 1H), 7.89 (s, 2H), 8.41 (d, *J* = 2.4, 1H); δ_C (100 MHz, DMSO-d_6): 21.7, 22.2, 120.7, 127.9, 128.7, 129.4, 134.5, 138.7, 156.2, 159.5, 161.6; ESI-HRMS (m/z) $[M-H]^-$: calculated for $C_{14}H_{15}ClN_3O_9S$ 436.0212; found 436.0208.

3,4-Dihydroxy-5-nitro-benzenesulfonamide (12).

$NaNO_2$ (1.2 eq) was added portion wise to a solution of 3-amino-4-hydroxy-5-nitro-benzenesulfonamide **8** (0.06 g, 1.0 eq) in HCl 2M (4 ml) at 0°C and that was stirred at r.t. for 15 min. The reaction mixture was extracted with EtOAc (3x10), the organic layers were dried over Na_2SO_4, filtered-off and concentrated under *vacuo* to give a residue that was purified by silica gel column chromatography eluting with MeOH/DCM 15% to afford the titled compound **12** as a brown solid**.** 60% yield; m.p. 200°C dec.; silica gel TLC R_f 0.21 (MeOH/DCM 10 % *v/v*); δ_H (400 MHz, DMSO-d_6): 7.56 (s, 2H, exchange with D_2O, SO_2NH_2) 8.59 (d, *J* = 2.6, 1H), 8.71 (d, *J* = 2.6, 1H); δ_C (100 MHz, DMSO-d_6): 98.3, 125.6, 137.4, 135.7, 142.6, 165.7; ESI-HRMS (m/z) $[M-H]^-$: calculated for $C_6H_5N_2O_6S$ 232.9863; found 232.9861.

General synthetic procedure of 4-hydroxy-3-nitro-5-ureido-benzenesulfonamides 13-25.[29]

The proper isocyanate (1.1 eq) was added to a suspension of 3-amino-4-hydroxy-5-nitro-benzenesulfonamide **8** (0.06 g, 1.0 eq) in dry CH_3CN (1.5 ml) under a nitrogen atmosphere and that was stirred at r.t. until starting material was consumed (TLC monitoring). The solvent was removed under *vacuo* and the obtained residue was purified by silica gel column chromatography eluting with MeOH/DCM from 5 to 15%.

4-Hydroxy-3-nitro-5-(3-phenyl-ureido)-benzenesulfonamide (13).

Compound **13** was obtained according the general procedure earlier reported using 3-amino-4-hydroxy-5-nitro-benzenesulfonamide **8** (0.06 g, 1.0 eq) and phenyl isocyanate (1.1eq) in dry CH_3CN (1.5 ml). The reaction mixture was stirred at r.t. overnight to afford the titled compound **13** as a red solid. 80% yield; m.p. 225-227°C; silica gel TLC R_f 0.40 (MeOH/DCM 20 % *v/v*); δ_H (400 MHz, DMSO-d_6): 7.05 (t, *J* = 7.6, 1H), 7.35 (t, *J* = 7.6, 2H), 7.51 (d, *J* = 7.6, 2H), 7.52 (s, 2H, exchange with D_2O, SO_2NH_2), 8.04 (d, *J* = 2.4, 1H), 8.84 (s, 1H, exchange with D_2O, N*H*CO), 8.99 (d, *J* = 2.4, 1H), 9.66 (s, 1H, exchange with D_2O, N*H*CO); δ_C (100 MHz, DMSO-d_6): 115.8, 119.1, 119.6, 123.2, 129.7, 129.9, 133.6, 134.9, 135.6, 140.3, 153.1; ESI-HRMS (m/z) $[M-H]^-$: calculated for $C_{13}H_{11}N_4O_6S$ 351.0394; found 351.0387.

3-[3-(4-Fluoro-phenyl)-ureido]-4-hydroxy-5-nitro-benzenesulfonamide (14).

Compound **14** was obtained according the general procedure earlier reported using 3-amino-4-hydroxy-5-nitro-benzenesulfonamide **8** (0.06 g, 1.0 eq) and 4-F-phenyl isocyanate (1.1 eq) in dry CH_3CN (1.5 ml). The reaction mixture was stirred at r.t. overnight to afford the titled compound **14** as a red solid. 84% yield; m.p. 250°C dec.; silica gel TLC R_f 0.26 (MeOH/DCM 20 % *v/v*);δ_H (400 MHz, DMSO-d_6): 6.92 (s, 2H, exchange with D_2O, SO_2NH_2), 7.13 (t, *J* = 8.8, 2H), 7.51 (m, 2H), 7.93 (d, *J* = 2.4, 1H), 8.33 (d, *J* = 2.4, 1H), 8.91 (s, 1H, exchange with D_2O, N*H*CO), 9.73 (s, 1H,

exchange with D_2O, N*H*CO); δ_F (376 MHz, DMSO-d_6): -121.99 (s, 1F); δ_C (100 MHz, DMSO-d_6): 113.2, 116.2 (d, J^2CF = 22.0), 118.9, 120.6 (d, J^3CF = 7.0), 122.6, 132.5, 136.9, 137.4, 153.4, 158.1 (d, J^1CF = 236.0), 160.9; ESI-HRMS (m/z) $[M-H]^-$: calculated for $C_{13}H_{10}FN_4O_6S$ 369.0300; found 369.0295.

4-Hydroxy-3-nitro-5-[3-(4-trifluoromethyl-phenyl)-ureido]-benzenesulfonamide (15).

Compound **15** was obtained according the general procedure earlier reported using 3-amino-4-hydroxy-5-nitro-benzenesulfonamide **8** (0.06 g, 1.0 eq) and 4-CF_3-phenyl isocyanate (1.1eq) in dry CH_3CN (1.5 ml). The reaction mixture was stirred at r.t. overnight to afford **15** as a red solid. 75% yield; m.p. 225-226°C; silica gel TLC R_f 0.13 (MeOH/DCM 10 % *v/v*);δ_H (400 MHz, DMSO-d_6): 6.94 (s, 2H, exchange with D_2O, SO_2NH_2), 7.65 (d, *J* = 8.8, 2H), 7.72 (d, *J* = 8.8, 2H), 7.96 (d, *J* = 2.4, 1H), 8.36 (d, *J* = 2.4, 1H), 9.04 (s, 1H, exchange with D_2O, N*H*CO), 10.11 (s, 1H, exchange with D_2O, N*H*CO); δ_F (376 MHz, DMSO-d_6): -59.99 (s, 3F); δ_C (100 MHz, DMSO-d_6): 113.7, 118.6, 119.2, 122.3 (q, J^2CF = 31.8), 122.7, 122.9 (q, J^1CF = 270.0), 126.9 (q, J^3CF = 3.7), 132.6, 136.5, 144.8, 153.1, 160.8; ESI-HRMS (m/z) $[M-H]^-$: calculated for $C_{14}H_{10}F_3N_4O_6S$ 419.0268; found 419.0276.

3-[3-(4-Fluoro-3-methyl-phenyl)-ureido]-4-hydroxy-5-nitro-benzenesulfonamide (16).

Compound **16** was obtained according the general procedure earlier reported using 3-amino-4-hydroxy-5-nitro-benzenesulfonamide **8** (0.06 g, 1.0 eq) and 4-F-3-methyl phenyl isocyanate (1.1 eq) in dry CH_3CN (1.5 ml). The reaction mixture was stirred at r.t. overnight to afford **16** as a red solid. 81% yield; m.p. 240°C dec.; silica gel TLC R_f 0.27 (MeOH/DCM 20 % *v/v*); δ_H (400 MHz, DMSO-d_6): 2.42 (d, *J* = 1.2, 3H, CH_3), 6.87 (s, 2H, exchange with D_2O, SO_2NH_2), 7.05 (t, *J* = 9.2, 1H), 7.28 (m, 1H), 7.45 (m, 1H), 7.93 (d, *J* = 2.4, 1H), 8.30 (d, *J* = 2.4, 1H), 8.87 (s, 1H, exchange with D_2O, N*H*CO), 9.63 (s, 1H, exchange with D_2O, N*H*CO); δ_F (376 MHz, DMSO-d_6): -126.41 (s, 1F); δ_C (100 MHz, DMSO-d_6): 15.4 (d, J^3CF = 3.0), 112.6, 115.7 (d, J^2CF = 22.8), 117.9 (d, J^3CF = 7.6),

118.9, 121.9 (d, J^3CF = 4.2), 122.0, 124.9 (d, J^2CF = 17.8), 132.7, 137.0, 131.1, 153.4, 156.7 (d, J^1CF = 236.0), 161.7; ESI-HRMS (m/z) $[M-H]^-$: calculated for $C_{14}H_{12}FN_4O_6S$ 383.0456; found 383.0461.

4-Hydroxy-3-nitro-5-(3-pentafluorophenyl-ureido)-benzenesulfonamide (17).

Compound **17** was obtained according the general procedure earlier reported using 3-amino-4-hydroxy-5-nitro-benzenesulfonamide **8** (0.06 g, 1.0 eq) and pentafluorophenyl isocyanate (1.1 eq) in dry CH_3CN (1.5 ml). The reaction mixture was stirred at r.t. overnight to afford **17** as a red solid. 79% yield; m.p. 250°C dec.; silica gel TLC R_f 0.31 (MeOH/DCM 20 % *v/v*); δ_H (400 MHz, DMSO-d_6): 7.01 (s, 2H, exchange with D_2O, SO_2NH_2), 7.98 (d, *J* = 2.2, 1H), 8.52 (d, *J* = 2.2, 1H), 9.88 (bs, 1H, exchange with D_2O, N*H*CO), 10.73 (bs, 1H, exchange with D_2O, N*H*CO); δ_F (376 MHz, DMSO-d_6): -164.84 (t, *J* = 22.6, 2F), -160.02 (t, *J* = 22.6, 1F), -145.82 (d, *J* = 22.6, 2F); ESI-HRMS (m/z) $[M-H]^-$: calculated for $C_{13}H_6F_5N_4O_6S$ 440.9923; found 440.9930.

4-Hydroxy-3-[3-(3-methoxy-phenyl)-ureido]-5-nitro-benzenesulfonamide (18).

Compound **18** was obtained according the general procedure earlier reported using 3-amino-4-hydroxy-5-nitro-benzenesulfonamide **8** (0.06 g, 1.0 eq) and 3-methoxy phenyl isocyanate (1.1 eq) in dry CH_3CN (1.5 ml). The reaction mixture was stirred at r.t. overnight to afford **18** as a red solid. 71% yield; m.p. 255°C dec.; silica gel TLC R_f 0.15 (MeOH/DCM 10 % *v/v*); δ_H (400 MHz, DMSO-d_6): 3.78 (s, 3H, OC*H*$_3$), 6.64 (dd, *J* = 2.4,7.8, 1H), 6.97 (dd, *J* = 2.4, 7.8, 1H), 7.24 (t, *J* = 7.8, 1H), 7.26 (s, 1H), 7.51 (s, 2H, exchange with D_2O, SO_2NH_2), 8.03 (d, *J* = 2.2, 1H), 8.40 (s, 1H, exchange with D_2O, N*H*CO), 8.97 (d, *J* = 2.2, 1H), 9.68 (s, 1H, exchange with D_2O, N*H*CO); δ_C (100 MHz, DMSO-d_6): 55.8, 104.5, 108.1, 111.2, 113.1, 118.9, 122.4, 130.4, 132.4, 136.9, 142.4, 153.3, 160.6, 161.2; ESI-HRMS (m/z) $[M-H]^-$: calculated for $C_{14}H_{13}N_4O_7S$ 381.0499; found 381.0503.

3-(3-Benzo[1,3]dioxol-5-yl-ureido)-4-hydroxy-5-nitro-benzenesulfonamide (19).

Compound **19** was obtained according the general procedure earlier reported using 3-amino-4-hydroxy-5-nitro-benzenesulfonamide **8** (0.06 g, 1.0 eq) and 5-isocyanato-benzo[1,3]dioxole (1.1 eq) in dry CH_3CN (1.5 ml). The reaction mixture was stirred at r.t. overnight to afford **19** as a red solid**.** 78% yield; m.p. 225-228°C; silica gel TLC R_f 0.21 (MeOH/DCM 10 % *v/v*); δ_H (400 MHz, DMSO-d_6): 6.02 (s, 2H, CH_2), 6.79 (dd, *J* = 2.0, 8.4, 1H), 6.89 (d, *J* = 8.4, 1H), 7.27 (d, *J* = 2.0, 1H), 7.51 (s, 2H, exchange with D_2O, SO_2NH_2), 8.01 (d, *J* = 2.2, 1H), 8.76 (s, 1H, exchange with D_2O, N*H*CO), 8.96 (d, *J* = 2.2, 1H), 9.55 (s, 1H, exchange with D_2O, N*H*CO); δ_C (100 MHz, DMSO-d_6): 101.7, 101.9, 109.2, 112.0, 115.5, 120.1, 133.3, 134.5, 135.8, 135.6, 143.4, 145.1, 148.3, 153.1; ESI-HRMS (m/z) $[M-H]^-$: calculated for $C_{14}H_{11}N_4O_8S$ 395.0292; found 395.0289.

3-[3-(3,5-Dimethyl-phenyl)-ureido]-4-hydroxy-5-nitro-benzenesulfonamide (20).

Compound **20** was obtained according the general procedure earlier reported using 3-amino-4-hydroxy-5-nitro-benzenesulfonamide **8** (0.06 g, 1.0 eq) and 3,5-dimethylphenyl isocyanate (1.1 eq) in dry CH_3CN (1.5 ml). The reaction mixture was stirred at r.t. overnight to afford **20** as a red solid. 82% yield; m.p. 215°C dec.; silica gel TLC R_f 0.54 (MeOH/DCM 20 % *v/v*); δ_H (400 MHz, DMSO-d_6): 2.26 (s, 6H, 2 x CH_3), 6.62 (s, 1H), 6.91 (s, 2H, exchange with D_2O, SO_2NH_2), 7.15 (s, 2H), 7.93 (d, *J* = 2.8, 1H), 8.36 (d, *J* = 2.8, 1H), 8.88 (s, 1H, exchange with D_2O, N*H*CO), 9.52 (s, 1H, exchange with D_2O, N*H*CO); δ_C (100 MHz, DMSO-d_6): 22.1, 113.4, 116.8, 118.6, 123.0, 124.1, 132.5, 36.9, 138.5, 140.9, 153.4, 160.6; ESI-HRMS (m/z) $[M-H]^-$: calculated for $C_{15}H_{15}N_4O_6S$ 379.0707; found 379.0706.

3-[3-(3,5-Bis-trifluoromethyl-phenyl)-ureido]-4-hydroxy-5-nitro-benzenesulfonamide (21).

Compound **21** was obtained according the general procedure earlier reported using 3-amino-4-hydroxy-5-nitro-benzenesulfonamide **8** (0.06 g, 1.0 eq) and 3,5-bis-trifluoromethylphenyl isocyanate (1.1 eq) in dry CH_3CN (1.5 ml). The reaction mixture was stirred at r.t. overnight to afford **21** as a red solid. 80% yield; m.p. 245°C dec.; silica gel TLC R_f 0.14 (MeOH/DCM 10 %

v/v); δ_H (400 MHz, DMSO-d_6): 6.97 (s, 2H, exchange with D_2O, SO_2NH_2), 7.65 (s, 1H), 7.98 (d, J = 2.8, 1H), 8.15 (s, 2H), 8.37 (d, J = 2.8, 1H), 9.16 (s, 1H, exchange with D_2O, N*H*CO), 10.54 (s, 1H, exchange with D_2O, N*H*CO); δ_F (376 MHz, DMSO-d_6): -61.72 (s, 6F); δ_C (100 MHz, DMSO-d_6): 113.8, 114.9, 118.6, 119.5, 122.2, 124.3 (q, J^1CF = 270.9), 131.6 (q, J^2CF = 32.3), 132.5, 136.4, 143.1, 153.2, 161.6; ESI-HRMS (m/z) $[M-H]^-$: calculated for $C_{15}H_9F_6N_4O_6S$ 487.0142; found 487.0143.

4-Hydroxy-3-nitro-5-(3-phenethyl-ureido)-benzenesulfonamide (22).

Compound **2** was obtained according the general procedure earlier reported using 3-amino-4-hydroxy-5-nitro-benzenesulfonamide **8** (0.06 g, 1.0 eq) and phenethyl isocyanate (1.1eq) in dry CH_3CN (1.5 ml). The reaction mixture was stirred at r.t. overnight to afford **22** as a red solid. 62% yield; m.p. 245-248°C; silica gel TLC R_f 0.10 (MeOH/DCM 5 % *v/v*);δ_H (400 MHz, DMSO-d_6): 2.77 (t, J = 7.6, 2H, CH_2), 3.30 (t, J = 7.6, 2H, overlap with water signal, CH_2), 6.87 (s, 2H, exchange with D_2O, SO_2NH_2), 7.28 (m, 5H), 7.90 (d, J = 2.2, 1H), 7.96 (s, 1H, exchange with D_2O, N*H*CO), 8.38 (d, J = 2.2, 1H), 8.91 (s, 1H, exchange with D_2O, N*H*CO); δ_C (100 MHz, DMSO-d_6): 37.4, 41.8, 112.3, 118.0, 122.6, 126.9, 129.2, 129.6, 132.2, 138.1, 140.8, 156.3, 161.8; ESI-HRMS (m/z) $[M-H]^-$: calculated for $C_{15}H_{15}N_4O_6S$ 379.0707; found 379.0702.

3-(3-Furan-2-ylmethyl-ureido)-4-hydroxy-5-nitro-benzenesulfonamide (23).

Compound **23** was obtained according the general procedure earlier reported using 3-amino-4-hydroxy-5-nitro-benzenesulfonamide **8** (0.06 g, 1.0 eq) and furfuryl isocyanate (1.1eq) in dry CH_3CN (1.5 ml). The reaction mixture was stirred at r.t. overnight to afford **23** as a red solid. 44% yield; m.p. 223-226°C; silica gel TLC R_f 0.12 (MeOH/DCM 5 % *v/v*);δ_H (400 MHz, DMSO-d_6): 4.33 (d, J = 5.6, 2H, CH_2), 6.22 (s, 1H, Ar-*H*), 6.39 (s, 1H, Ar-*H*), 6.86 (s, 2H, exchange with D_2O, SO_2NH_2), 7.56 (s, 1H, Ar-*H*), 7.89 (d, J = 2.4, 1H, Ar-*H*), 8.19 (bs, 1H, exchange with D_2O, N*H*CO), 8.34 (d, J = 2.4, 1H, Ar-*H*), 8.94 (s, 1H, exchange with D_2O, N*H*CO); δ_C (100 MHz,

DMSO-d_6): 36.9, 106.8, 111.3, 112.8, 118.1, 123.0, 132.3, 138.0, 142.4, 155.2, 156.3, 161.5; ESI-HRMS (m/z) $[M-H]^-$: calculated for $C_{12}H_{11}N_4O_7S$ 355.0343; found 355.0339.

(2S,3S,4S,5R,6S)-6-(acetoxymethyl)-3-(3-(2-hydroxy-3-nitro-5-sulfamoylphenyl)ureido)tetrahydro-2H-pyran-2,4,5-triyl triacetate (24).

Compound **24** was obtained according the general procedure earlier reported using 3-amino-4-hydroxy-5-nitro-benzenesulfonamide **8** (0.06 g, 1.0 eq) and acetic acid 2,5-diacetoxy-6-acetoxymethyl-3-isocyanato-tetrahydro-pyran-4-yl ester **26** (3.0 eq) in dry CH_3CN (1.5 ml). The reaction mixture was stirred at r.t. for 48h to afford **24** as a red solid. 63% yield; m.p. 191-194°C; silica gel TLC R_f 0.20 (MeOH/DCM 10 % *v/v*); δ_H (400 MHz, DMSO-d_6): 1.92 (s, 3H, COCH_3), 2.02 (s, 3H, COCH_3), 2.06 (s, 3H, COCH_3), 2.06 (s, 3H, COCH_3), 3.90 (m, 1H, C*H*), 4.05 (m, 2H, 2 x C*H*), 4.24 (dd, *J* = 4.4, 12.4, 1H, C*H*), 4.94 (t, *J* = 9.6, 1H, C*H*), 5.36 (m, 1H, C*H*), 5.92 (m, 1H, C*H*), 6.97 (s, 2H, exchange with D_2O, SO_2NH_2), 7.74 (bs, 1H, exchange with D_2O, N*H*CO), 7.92 (d, *J* = 2.6, 1H, Ar-*H*), 8.36 (d, *J* = 2.6, 1H, Ar-*H*), 8.79 (bs, 1H, exchange with D_2O, N*H*CO); δ_C (100 MHz, DMSO-d_6): 21.3, 21.4, 21.5, 21.6, 55.8, 62.6, 69.4, 72.4, 73.1, 93.0, 113.7, 118.2, 124.0, 132.6, 137.1, 155.8, 160.1, 169.9, 170.3, 170.5, 171.0; ESI-HRMS (m/z) $[M-H]^-$: calculated for $C_{21}H_{25}N_4O_{15}S$ 605.1032; found 605.1033.

4-Hydroxy-3-nitro-5-(3-((3S,4S,5R,6S)-2,4,5-trihydroxy-6-(hydroxymethyl)tetrahydro-2H-pyran-3-yl)ureido)benzenesulfonamide (25).

Compound **24** (0.04g, 1.0 eq) was added to a freshly prepared sodium methoxide (7.0 eq) methanolic solution (5 ml) under a nitrogen atmosphere at 0°C and that was stirred at 0°C for 0.5h. Neutralization of the solution with Amberlite IR-120-H^+ ion exchange resin, followed by filtration (the resin washed several times with methanol) and evaporation of the filtrate to dryness, afforded compound **25**.74% yield; ESI-HRMS (m/z) $[M-H]^-$: calculated for $C_{13}H_{17}N_4O_{11}S$ 437.0609; found 437.0611.

4.2. CA inhibition

An Applied Photophysics stopped-flow instrument has been used for assaying the CA catalysed CO_2 hydration activity.[49] Phenol red (at a concentration of 0.2 mM) has been used as indicator, working at the absorbance maximum of 557 nm, with 20 mM Hepes (pH 7.5) as buffer, and 20 mM Na_2SO_4 (for maintaining constant the ionic strength), following the initial rates of the CA-catalyzed CO_2 hydration reaction for a period of 10-100 s. The CO_2 concentrations ranged from 1.7 to 17 mM for the determination of the kinetic parameters and inhibition constants. For each inhibitor at least six traces of the initial 5-10% of the reaction have been used for determining the initial velocity. The uncatalyzed rates were determined in the same manner and subtracted from the total observed rates. Stock solutions of inhibitor (0.1 mM) were prepared in distilled-deionized water and dilutions up to 0.01 nM were done thereafter with the assay buffer. Inhibitor and enzyme solutions were preincubated together for 15 min at room temperature prior to assay, in order to allow for the formation of the E-I complex. The inhibition constants were obtained by non-linear least-squares methods using PRISM 3 and the Cheng-Prusoff equation, as reported earlier,[57] and represent the mean from at least three different determinations. All CA isofoms were recombinant ones obtained in-house as reported earlier.[58,59]

X-ray Crystallography

CA II and CA IX/mimic were transformed in *E. coli* BL21 (DE3) competent cells in Luria broth medium containing 100mg/ml of Ampicillin at 37℃. CA IX/mimic is a CA II variant with seven amino acid substitutions (A65S, N67Q, E69T, I91L, F131V, K170E and L204A) in the active site to mimic that of CA IX. Protein expression was induced by 0.1mg/ml isopropyl β-D thiogalactoside (IPTG). After incubating for 3 h at 37℃, the cells were harvested by centrifugation. Purification

was performed using a *p*-aminomethyl-benzenesulfonamide agarose affinity column and the protein eluted with 400mM sodium azide, 50 mM Tris, pH 7.8. Both CA II and CA IX/mimic were buffer exchanged (into 50mM Tris-HCl, pH 7.8) and concentrated using Amicon ultra-filtration centrifugal tubes with a 10 kDa molecular weight cut-off. Purity was verified by SDS-PAGE stained with coomassie brilliant blue and concentration determined by UV spectroscopy at 280 nm with a molar extinction coefficient of 54800 cm^{-1} mol^{-1}.

The CA II and CA IX/mimic crystals were grown via the hanging drop vapor diffusion method with a precipitant solution of 1.6 M sodium citrate, 50 mM Tris and pH 7.8 at room temperature (RT). Crystal drops were set up in a 1:1 ratio with 2.5µl of protein and 2.5 µl of precipitant solution. The stock concentrations of CA II and CA IX/mimic were 10 mg/ml, resulting in a final concentration of 5 mg/ml protein in the drop.

The inhibitors were dissolved in 100% dimethyl sulfoxide (DMSO) and then diluted 10-fold in the precipitant solution to a final concentration of 1.2, 1.3 and 1.1 mM for **15**, **16** and **17**, respectively. The CA II and CA IX/mimic crystals were soaked overnight with the inhibitors.

X-ray diffraction data were collected at RT in-house using a Rigaku RU-H3R rotating Cu anode (wavelength of 1.5418 Å) operating at 50 kV and 22 mA with osmic mirrors and an R-Axis IV^{++} image detector. A total of 180 images were collected for each data set with a crystal to detector distance of 100 mm, exposure time of 10 min, and oscillation angle of 1°. Data collection was performed at RT. The data were indexed and integrated using the HKL2000 software package.[60] Molecular replacement was used for initial phasing in PHENIX (Phaser-MR One-Component Interface) [61] using CAII (PDB ID: 3KS3) as a search model.[62] The model refinements and generation of ligand restraint files were also performed using the PHENIX programs. COOT (Crystallographic object oriented toolkit) [63] was utilized to observe refinements and evaluate the structure. The percentage of inhibitor-bound surface area was calculated using PDB e-PISA.[64] All the figures were generated using PyMol.[65]

Cell culture and treatments

Human prostate cancer cell line PC3, human breast cancer cell line MDA-MB-231, and human colon cancer cell line HT-29 were obtained from American Type Culture Collection (Rockville, MD). PC3, MDA-MB-231 and HT-29 were cultured in DMEM high glucose with 20% FBS in 5% CO_2 atmosphere at 37° C. Media contained 2 mM L-glutamine, 1% essential amino acid mix, 100 IU ml-1 penicillin and 100 µg ml^{-1} streptomycin (Sigma, Milan, Italy). Cells were plated in 96-wells cell culture (1.104/well) and, 24 h after, treated with the tested compounds (0-200 µM) for 48 h. Low oxygen conditions were acquired in a hypoxic workstation (Concept 400 anaerobic incubator, Ruskinn Technology Ltd., Bridgend, UK). The atmosphere in the chamber consisted of 1% O_2 (hypoxia), 5% CO_2, and residual N_2. In parallel, normoxic (20% O_2) dishes were incubated in air with 5% CO_2.

Cell viability assay

PC3, MDA-MB-231 and HT-29 cell viability was evaluated by the reduction of 3-(4,5-dimethylthiozol-2-yl)-2,5-diphenyltetrazolium bromide (MTT) as an index of mitochondrial compartment functionality. Cells were plated and treated as described. Post-treatments, after extensive washing, 1 mg/ml MTT was added into each well and incubated for 30 minutes at 37 °C. After washing, the formazan crystals were dissolved in 150 µl DMSO. The absorbance was measured at 550 nm. Experiments were performed in quadruplicate on at least three different cell batches.

Statistical analysis

Results were expressed as mean ± S.E.M. and the analysis of variance was performed by one way ANOVA. A Bonferroni's significant difference procedure was used as post-hoc comparison. *P* values of less than 0.05 were considered as significant. Data were analyzed using the "Origin® 9.1" software.

Acknowledgment

Ente Cassa di Risparmio di Firenze, Italy, is gratefully acknowledged for a grant to A.N (ECR 2016.0774). C.L.L. is supported by the National Center for Advancing Translational Sciences of the National Institutes of Health under University of Florida Clinical and Translational Science Awards TL1TR001428 and UL1TR001427. The content is solely the responsibility of the authors and does not necessarily represent the official views of the National Institutes of Health.

■ Supporting Information

The Supporting Information is available free of charge on the ACS Publications website at DOI: additional synthetic procedures and characterization of compounds, NMR spectra, HPLC-purity chromatograms, supplemental X-ray crystallographic figures, anti-proliferative assays data. SMILES representation for compounds (CSV).

■ ASSOCIATED CONTENT

Coordinates and structure factors for hCA II and hCA IX-mimic complexes with **15**, **16** and **17** have been deposited in the Protein Data Bank (PDB) with accession codes: hCAII_**15**: 6EBE, hCAII_**16**: 6EDA, hCAII_**17**: 6ECZ, CA IX-mimic_**15**: 6EEA, CA IX-mimic_**16**: 6EEO, A CA IX-mimic_**17**: 6EEH. Authors will release the atomic coordinates and experimental data upon article publication.

■ ABBREVIATIONS USED

HIF-1, hypoxia-inducible factor 1; HAP, hypoxia-activated prodrug; CA, carbonic anhydrase; CAI, CA inhibitor; K_I, inhibition constant; Boc, tert-butyloxycarbonyl; EtOAc, ethyl acetate; DMF, dimethyl formamide; DCM, dichloromethane; MeOH, methanol.

■ AUTHOR INFORMATION

*Corresponding Author:

Phone: +39-055-4573685. E-mail: alessio.nocentini@unifi.it (AN)

Phone: +39-055-4573701. Email: paola.gratteri@unifi.it (PG)

Phone: +39-055-4573729. Fax: +39-055-4573385. E-mail: claudiu.supuran@unifi.it (CTS)

References

1. Wilson, W.R.; Hay, M.P. Targeting hypoxia in cancer therapy. *Nat. Rev. Cancer.* **2011**, *11*, 393-410.

2. Taddei, M.L.; Giannoni, E.; Comito, G.; Chiarugi, P. Microenvironment and tumor cell plasticity: an easy way out. *Cancer Lett.* **2013**, *341*, 80–96.

3. Finger, E.C.; Giaccia, A.J. Hypoxia, inflammation, and the tumor microenvironment in metastatic disease. *Cancer Metastasis Rev.* **2010**, *29*, 285–293.

4. Semenza, G.L. Regulation of cancer cell metabolism by hypoxia inducible factor 1. *Semin. Cancer Biol.* **2009**, *19*.12-16.

5. Gatenby, R.A.; Gillies, R.J. Why do cancers have high aerobic glycolysis? *Nat. Rev. Cancer.* **2004**, *4*, 891-899.

6. Neri, D.; Supuran, C.T. Interfering with pH regulation in tumours as a therapeutic strategy. *Nat. Rev. Drug Discov.* **2011**, *10*, 767-777.

7. Graeber, T.G.; Osmanian, C.; Jacks, T.; Housman, D.E.; Koch, C.J.; Lowe, S.W.; Giaccia, A.J. Hypoxia-mediated selection of cells with diminished apoptotic potential in solid tumours. *Nature* **1996**, *379*, 88-91.

8. Chan, N.; Koritzinsky, M.; Zhao, H.; Bindra, R.; Glazer, P.M.; Powell, S.; Belmaaza, A.; Wouters, B.; Bristow, R.G. Chronic hypoxia decreases synthesis of homologous recombination proteins to offset chemoresistance and radioresistance. *Cancer Res.* **2008**, *68*, 605-614.

9. Axelson, H.; Fredlund, E.; Ovenberger, M.; Landberg, G.; Pahlman, S. Hypoxia-induced dedifferentiation of tumor cells – a mechanism behind heterogeneityand aggressiveness of solid tumors. *Semin. Cell. Dev. Biol.* **2005**, *16*, 554–563.

10. Dubois, L.; Peeters, S.; Lieuwes, N.G.; Geusens, N.; Thiry, A.; Wigfield, S.; Carta, F.; McIntyre, A.; Scozzafava, A.; Dogné, J.M.; Supuran, C.T.; Harris, A.L.; Masereel, B.; Lambin, P. Specific inhibition of carbonic anhydrase IX activity enhances the in vivo therapeutic effect of tumor irradiation. *Radiother. Oncol.* **2011**, *99*, 424–431.

11. Guise, C.P.; Mowday, A.M.; Ashoorzadeh, A.; Yuan, R.; Lin, W.; Wu, D.; Smaill, J.B.; Patterson, A.V.; Ding. K. Bioreductive prodrugs as cancer therapeutics: targeting tumor hypoxia. *Chin. J. Cancer* **2014**, *33*, 80-86.

12. Baran, N.; Konopleva, M. Molecular pathways: hypoxia-activated prodrugs in cancer therapy. *Clin. Cancer Res.* **2017**, *23*, 2382-2390.

13. Lindner, H.L. Hypoxia-activated prodrug: an appealing preclinical concept yet lost in clinical translation. *Lancet Oncol.* **2017**, *18*, 991-993.

14. Phillips, R.M. Targeting the hypoxic fraction of tumours using hypoxia-activated prodrugs. *Cancer Chemother. Pharmacol*. **2016**, *77*, 441–457.

15. Parliament, M.B.; Wiebe, L.I.; Franko, A.J. Nitroimidazole adducts as markers for tissue hypoxia: mechanistic studies in aerobic normal tissues and tumour cells. *Br. J. Cancer* **1992**, *66*, 1103–1108.

16. Patterson, A.V.; Ferry, D.M.; Edmunds, S.J.; Gu, Y.; Singleton, R.S.; Patel, K.; Pullen, S.M.; Hicks, K.O.; Syddall, S.P.; Atwell, G.J.; Yang, S.; Denny, W.A.; Wilson, W.R. Mechanism of action and preclinical antitumor activity of the novel hypoxia-activated DNA crosslinking agent PR-104. *Clin. Cancer Res.* **2007**,*13*, 3922- 3932.

17. Singleton, R.S.; Guise, C.P.; Ferry, D.M.; Pullen, S.M.; Dorie, M.J.; Brown, J.M.; Patterson, A.V.; Wilson, W.R. DNA crosslinks in human tumor cells exposed to the prodrug PR-104A:

relationships to hypoxia, bioreductive metabolism and cytotoxicity. *Cancer Res.* **2009**, *69*, 3884-3891.

18. Alterio, V.; Di Fiore, A.; D'Ambrosio, K.; Supuran, C.T.; De Simone, G. Multiple binding modes of inhibitors to carbonic anhydrases: how to design specific drugs targeting 15 different isoforms? *Chem. Rev*. **2012**, *112*, 4421-4468.

19. Supuran, C.T. Carbonic anhydrases: novel therapeutic applications for inhibitors and activators. *Nat. Rev. Drug. Discov.* **2008**, *7*, 168–181.

20. Supuran, C.T.; Alterio, V.; Di Fiore, A.; D' Ambrosio, K.; Carta, F.; Monti, S.M.; De Simone, G. Inhibition of carbonic anhydrase IX targets primary tumors, metastases, and cancer stem cells: Three for the price of one. *Med. Res. Rev.* **2018**, *38*, 1799-1836.

21. Alterio, V.; Hilvo, M.; Di Fiore, A.; Supuran, C.T.; Pan, P.; Parkkila, S.; Scaloni, A.; Pastorek, J.; Pastorekova, S.; Pedone, C.; Scozzafava, A.; Monti, S.M.; De Simone, G. Crystal structure of the catalytic domain of the tumor-associated human carbonic anhydrase IX. *Proc. Natl. Acad. Sci. U S A*. **2009**, *106*, 16233–16238.

22. Whittington, D.A.; Waheed, A; Ulmasov, B., Shah, G.N.; Grubb, J.H.; Sly, W.S.; Christianson, D.W. Crystal structure of the dimeric extracellular domain of human carbonic anhydrase XII, a bitopic membrane protein overexpressed in certain cancer tumor cells. *Proc. Natl. Acad. Sci. USA* **2001**, *98*, 9545-9550.

23. Supuran, C.T. How many carbonic anhydrase inhibition mechanisms exist. *J. Enzyme Inhib. Med. Chem.* **2016**, *31*, 345–360.

24. Ibrahim, H.S.; Allam, H.A.; Mahmoud, W.R.; Bonardi, A.; Nocentini, A.; Gratteri, P.; Ibrahim, E.S.; Abdel-Aziz, H.A.; Supuran, C.T. Dual-tail arylsulfone-based benzenesulfonamides differently match the hydrophobic and hydrophilic halves of human carbonic anhydrases active sites: Selective inhibitors for the tumor-associated hCA IX isoform. *Eur. J. Med. Chem.* **2018**, *152*, 1-9.

25. Scozzafava, A.; Menabuoni, L.; Mincione, F.; Briganti, F.; Mincione, G.; Supuran, C.T. Carbonic anhydrase inhibitors. Synthesis of water-soluble, topically effective, intraocular pressure-

lowering aromatic/heterocyclic sulfonamides containing cationic or anionic moieties: Is the tail more important than the ring? *J. Med. Chem.* **1999**, *42*, 2641−2650.

26. Bozdag, M.; Ferraroni, M.; Nuti, E.; Vullo, D.; Rossello, A.; Carta, F.; Scozzafava, A.; Supuran, C.T. Combining the tail and the ring approaches for obtaining potent and isoform-selective carbonic anhydrase inhibitors: solution and X-ray crystallographic studies. *Bioorg. Med. Chem.* **2014**, 22, 334−340.

27. Nocentini, A.; Ferraroni, M.; Carta, F.; Ceruso, M.; Gratteri, P.; Lanzi, C.; Masini, E.; Supuran, C. T. Benzenesulfonamides incorporating flexible triazole moieties are highly effective carbonic anhydrase inhibitors: synthesis and kinetic, crystallographic, computational, and intraocular pressure lowering investigations. *J. Med. Chem.* **2016**, *59*, 10692-10704.

28. Pacchiano, F.; Aggarwal, M.; Avvaru, B.S.; Robbins, A.H.; Scozzafava, A.; McKenna, R.; Supuran, C.T. Selective hydrophobic pocket binding observed within the carbonic anhydrase II active site accommodate different 4-substituted-ureido-benzenesulfonamides and correlate to inhibitor potency. *Chem. Commun.* **2010**, *46*, 8371–8373

29. Pacchiano, F.; Carta, F.; McDonald, P.C.; Lou, Y.; Vullo, D.; Scozzafava, A.; Dedhar, S.; Supuran, C.T. Ureido-substituted benzenesulfonamides potently inhibit carbonic anhydrase IX and show antimetastatic activity in amodel of breast cancer metastasis. *J. Med. Chem.* **2011**, *54*, 1896–1902.

30. Supuran C, Dedhar S, Mcdonald, M.C.; Carta, F. Novel Sulfonamide Compounds For Inhibition Of Metastatic Tumor Growth. WO021963; 2012.

31. Gieling, R.G.; Babur, M.; Mamnani, L.; Burrows, N.; Telfer, B.A.; Carta, F.; Winum, J.Y.; Scozzafava, A.; Supuran, C.T.; Williams, K.J. Antimetastatic effect of sulfamate carbonic anhydrase IX inhibitors in breast carcinoma xenografts. *J. Med. Chem.* **2012**, *55*, 5591–5600.

32. Carta, F.; Vullo, D.; Osman, S.M.; AlOthman, Z.; Supuran, C.T. Synthesis and carbonic anhydrase inhibition of a series of SLC-0111 analogs. *Bioorg. Med. Chem.* **2017**, *25*, 2569-2576.

33. Safety Study of SLC–0111 in Subjects With Advanced Solid Tumours. Available from https://clinicaltrials.gov/ct2/show/study/NCT02215850?term=SLC_0111&rank=1 (accessed June 18, 2018).

34. D'Ambrosio, K.; Vitale, R.M.; Dogné, J.M.; Masereel, B.; Innocenti, A.; Scozzafava, A.; De Simone, G.; Supuran, C.T. Carbonic anhydrase inhibitors: bioreductive nitro-containing sulfonamides with selectivity for targeting the tumor associated isoforms IX and XII. *J. Med. Chem.* **2008**, *51*, 3230-3237.

35. De Simone, G.; Vitale, R.M.; Di Fiore, A.; Pedone, C.; Scozzafava, A.; Montero, J.L.; Winum, J.Y.; Supuran, C.T. Carbonic anhydrase inhibitors: Hypoxia-activatable sulfonamides incorporating disulfide bonds that target the tumor-associated isoform IX. *J. Med. Chem.* **2006**, *49*, 5544-5551.

36. Rami, M.; Dubois, L.; Parvathaneni, N.K.; Alterio, V.; Van Kuijk, S.J.; Monti, S.M.; Lambin, P.; De Simone, G.; Supuran, C.T.; Winum, J.Y. Hypoxia-targeting carbonic anhydrase IX inhibitors by a new series of nitroimidazole-sulfonamides/sulfamides/sulfamates. *J. Med. Chem.* **2013**, *56*, 8512-8520.

37. Strauss, M.J. The nitroaromatic group in drug design. pharmacology and toxicology (for nonpharmacologists). *Ind. Eng. Chem. Prod. Res. Dev.*, **1979**, *18*, 158–166

38. Mori, M.; Cau, Y.; Vignaroli, G.; Laurenzana, I.; Caivano, A.; Vullo, D.; Supuran, C.T.; Botta M. Hit recycling: discovery of a potent carbonic anhydrase inhibitor by in silico target fishing. *ACS Chem. Biol.* **2015**, *10*, 1964-1969.

39. Bozdag, M.; Carta, F; Ceruso, M.; Ferraroni, M.; McDonald, P.C.; Dedhar, S.; Supuran, C.T. Discovery of 4-Hydroxy-3-(3-(phenylureido)benzenesulfonamides as SLC-0111 Analogues for the Treatment of Hypoxic Tumors Overexpressing Carbonic Anhydrase IX. *J. Med. Chem.* **2018**, *61*, 6328-6338.

40. Nocentini, A.; Vullo, D.; Bartolucci, G.; Supuran, C.T. N-Nitrosulfonamides: A new chemotype for carbonic anhydrase inhibition, *Bioorg. Med. Chem.* **2016**, *24*, 3612-3617.

41. Cai, L.; Han, Y.; Ren, S.; Huang, L. Dication C(R1)±N(R2)2 Synthons and their use in the Synthesis of Formamidines, Amidines, and a-Aminonitriles. *Tetrahedron* **2000**, *56*, 8253-8262.

42. Mitsugu, Y.D.; Leo, C.R.; Counde, O.; Francis, K.P. N-Phenyl-alkylsulfonamide Derivatives, Their Preparation And Their Use As Alpha 1A/1L Adrenoceptor Agonists. EP0887346; 2007.

43. Gamble, A.B.; Garner, J.; Gordon, C.P.; O'Conner, S.M.J. Aryl nitro reduction with iron powder or stannous chloride under ultrasonic irradiation. *Synth. Commun.* **2007**, *37*, 2777-2786.

44. Zulalian, J. Study of the absorption, excretion, metabolism, and residues in tissues in rats treated with carbon-14-labeled pendimethalin, PROWL herbicide. *J. Agric. Food Chem.* **1990**, *38*, 1743-1754.

45. Gotchev, D.B.; Jian, J; Yonghui, W. Prolyl Hydroxylase Inhibitors WO2010/059549; 2010.

46. Moreno-Fuquen, R. 2,4,6-Trinitrophenyl 4-bromobenzoate. *Acta Cryst.* **2013**, *E69*, o1787.

47. Supuran, C.T.; Scozzafava, A.; Ilies, M.A.; Iorga, B.; Cristea, T.; Briganti, F.; Chiraleu, F.; Banciu, M.D. Carbonic anhydrase inhibitors - Part 53. Synthesis of substituted-pyridinium derivatives of aromatic sulfonamides: The first non-polymeric membrane-impermeable inhibitors with selectivity for isozyme IV. *Eur J. Med. Chem.* **1998**, *33,* 577-594.

48. Ran, C.; Pantazopoulos, P.; Medarova, Z.; Moore. A. Synthesis and testing of beta-cell-specific streptozotocin-derived near-infrared imaging probes. *Angew. Chem. Int. Ed.* **2007**, *46*, 8998 –9001.

49. Lopez, O.; Maza, S.; Maya, I.; Fuentes, J.; Fernandez-Bolanos, J.G. New synthetic approaches to sugar ureas. Access to ureido-b-cyclodextrins. *Tetrahedron* **2005**, *61*, 9058–9069.

50. Khalifah, R.G. The carbon dioxide hydration activity of carbonic anhydrase. *J. Biol. Chem.* **1971**, *246*, 2561−2573.

51. Grandane, A.; Tanc, M.; Di Cesare Mannelli, L.; Carta, F.; Ghelardini, C.; Žalubovskis, R.; Supuran, C.T. 6-Substituted sulfocoumarins are selective carbonic anhdydrase IX and XII inhibitors with significant cytotoxicity against colorectal cancer cells. *J. Med. Chem.* **2015**, *58*, 3975-3983.

52. Angeli, A.; Tanini, D.; Peat, T.S.; Di Cesare Mannelli, L.; Bartolucci, G.; Capperucci, A.; Ghelardini, C.; Supuran, C.T.; Carta, F. Discovery of new selenoureido analogues of 4-(4-

fluorophenylureido)benzenesulfonamide as carbonic anhydrase inhibitors. *ACS Med. Chem. Lett.* **2017**, *8*, 963-968.

53. Bonardi, A.; Falsini, M.; Catarzi, D.; Varano, F.; Di Cesare Mannelli, L.; Tenci, B.; Ghelardini, C.; Angeli, A.; Supuran, C.T.; Colotta, V. Structural investigations on coumarins leading to chromeno[4,3-c]pyrazol-4-ones and pyrano[4,3-c]pyrazol-4-ones: New scaffolds for the design of the tumor-associated carbonic anhydrase isoforms IX and XII. *Eur. J. Med. Chem.* **2018**, *146*, 47-59.

54. Nocentini, A.; Bua, S.; Lomelino, C.L.; McKenna, R.; Menicatti, M.; Bartolucci, G.; Tenci, B.; Di Cesare Mannelli, L.; Ghelardini, C.; Gratteri, P.; Supuran, C.T. Discovery of new sulfonamide carbonic anhydrase IX inhibitors incorporating nitrogenous bases. *ACS Med. Chem. Lett.* **2017**, *8*, 1314-1319.

55. Marshall, A. G.; Hendrickson, C.L. High-resolution mass spectrometers. *Annu. Rev. Anal. Chem.* **2008**, *1*, 579-599.

56. Nocentini, A.; Ceruso, M.; Bua, S.; Lomelino, C.L.; Andring, J.T.; McKenna, R.; Lanzi, C.; Sgambellone, S.; Pecori, R.; Matucci, R.; Filippi, L.; Gratteri, P.; Carta, F.; Masini, E.; Selleri, S.; Supuran, C.T. Discovery of β-adrenergic receptors blocker-carbonic anhydrase inhibitor hybrids for multitargeted antiglaucoma therapy. *J. Med. Chem.* **2018**, *61*, 5380−5394.

57. Nocentini, A.; Moi, D.; Balboni, G.; Onnis, V.; Supuran, C.T. Discovery of thiazolin-4-one-based aromatic sulfamates as a new class of carbonic anhydrase isoforms I, II, IV, and IX inhibitors. *Bioorg Chem.* **2018**, *77*, 293-299

58. Leitans, J.; Kazaks, A.; Balode, A.; Ivanova, J.; Zalubovskis, R.; Supuran, C.T.; Tars, K. Efficient expression and crystallization system of cancer-associated carbonic anhydrase isoform IX. *J. Med. Chem.* **2015**, *58*, 9004-9009.

59. Nocentini, A.; Carta, F.; Tanc, M.; Selleri, S.; Supuran, C.T.; Bazzicalupi, C.; Gratteri, P. Deciphering the mechanism of human carbonic anhydrases inhibition with sulfocoumarins: computational and experimental studies. *Chemistry*. **2018**, *24*, 7840-7844

60. Otwinowski, Z.; Minor, W. Processing of X-ray Diffraction Data Collected in Oscillation Mode, Methods in Enzymology, Volume 276: Macromolecular Crystallography, part A, p.307-326, 1997, C.W. Carter, Jr. & R. M. Sweet, Eds., Academic Press (New York)

61. Adams, P.D.; Afonine, P.V.; Bunkoczi, G.; Chen, V.B.; Davis, I.W.; Echols, N.; Headd, J.J.; Hung, L.W.; Kapral, G.J.; Grosse-Kunstleve, R.W.; McCoy, A.J.; Moriarty, N.W.; Oeffner, R.; Read, R.J.; Richardson, D.C.; Richardson, J.S.; Terwilliger, T.C.; Zwart, P.H. PHENIX: a comprehensive Python-based system for macromolecular structure solution. *Acta Cryst.* **2010**, *D66*, 213-221.

62. Mikulski, R.; West, D.; Sippel, K.H.; Avvaru, B.S.; Aggarwal, M.; Tu, C.; Mckenna, R.; Silverman, D.N. Water networks in fast proton transfer during catalysis by human Carbonic Anhydrase II, *Biochemistry* **2013**, *49*, 125-131.

63.Emsley, P.; Cowtan, K. Coot: model-building tools for molecular graphics. *Acta Crystallogr.* **2004**, *D60*, 2126-2132.

64. 'Protein interfaces, surfaces and assemblies' service PISA at the European Bioinformatics Institute. (http://www.ebi.ac.uk/pdbe/prot_int/pistart.html), E. Krissinel and K. Henrick (2007).

65.The PyMol Molecular Graphics System, Version 1.5.0.4 Schrodinger, LLC.

Table of contents graphic

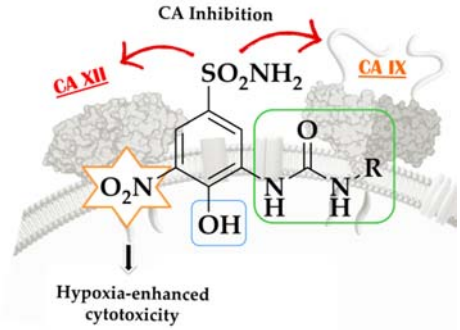

Caption: Bioreductive 4-hydroxy-3-nitro-5-ureido-benzenesulfonamides, designed on the anti-tumor phase II drug **SLC-0111**, selectively inhibit CA IX and XII and show hypoxia-enhanced anti-proliferative profiles.